Trapped Ion Liquids and Crystals

John Bollinger
NIST-Boulder
Ion storage group

Wayne Itano, David Wineland, Jospeh Tan, Pei Huang, Brana Jelenkovic, Travis Mitchell, Brad King, Jason Kriesel, Marie Jensen, Taro Hasegawa, Dan Dubin – UCSD(theory)

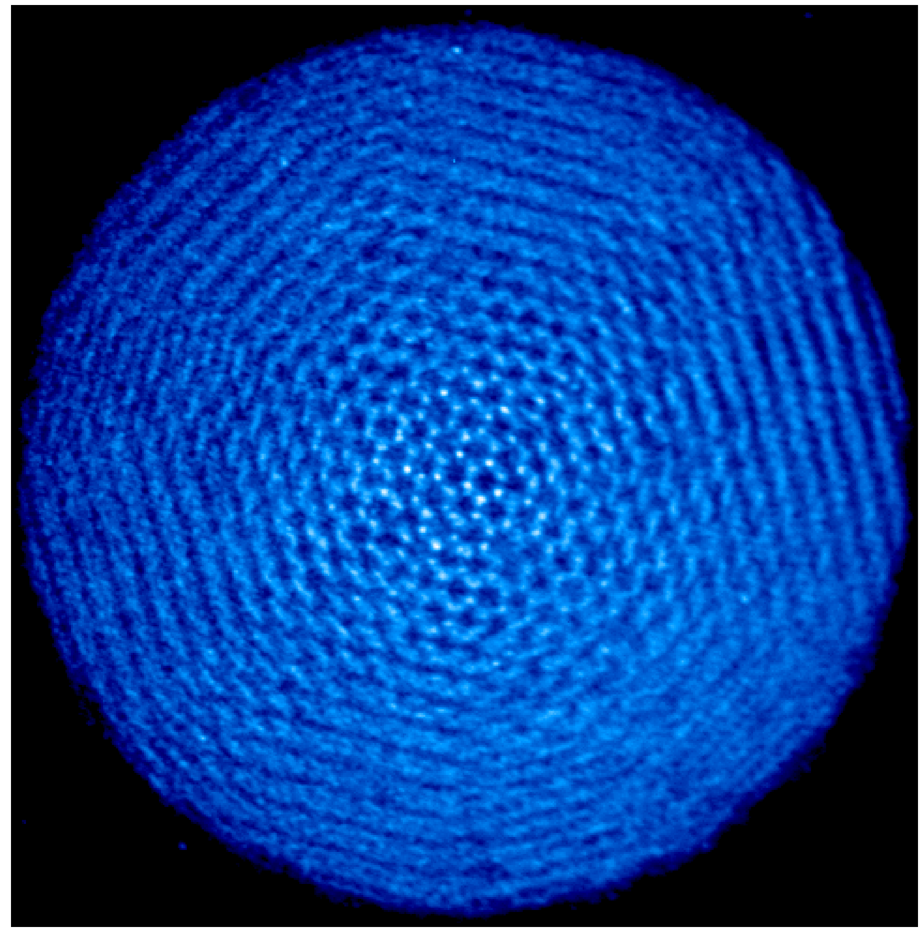

NIST National Institute of Standards and Technology

Department of the Navy ONR Science & Technology USN

Outline:

- Introduction:
  Penning traps, thermal equilibrium, one-component plasmas, strong correlation
- Observation of crystalline structure:
  Bragg scattering, real imaging, structural phase transitions
- Can we observe the predicted liquid-solid phase transition?
- Modes

→ No quantum mechanics; everything in this talk uses classical physics

→ Please ask questions!!

→ Ref: Dubin and O'Neil, Rev. Mod. Physics **71**, 87 (1999)

Types of traps in atomic physics

Rf or Paul Trap
RF & DC
Voltages

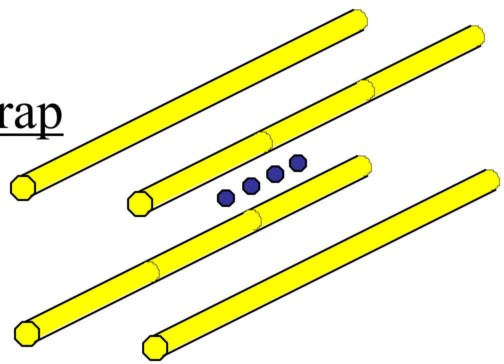

(see Wineland lectures)

good for tight confinement and laser cooling smaller numbers of particles

Penning Trap
(or Penning-
Malmberg trap)
DC Voltages &
Static B-Field

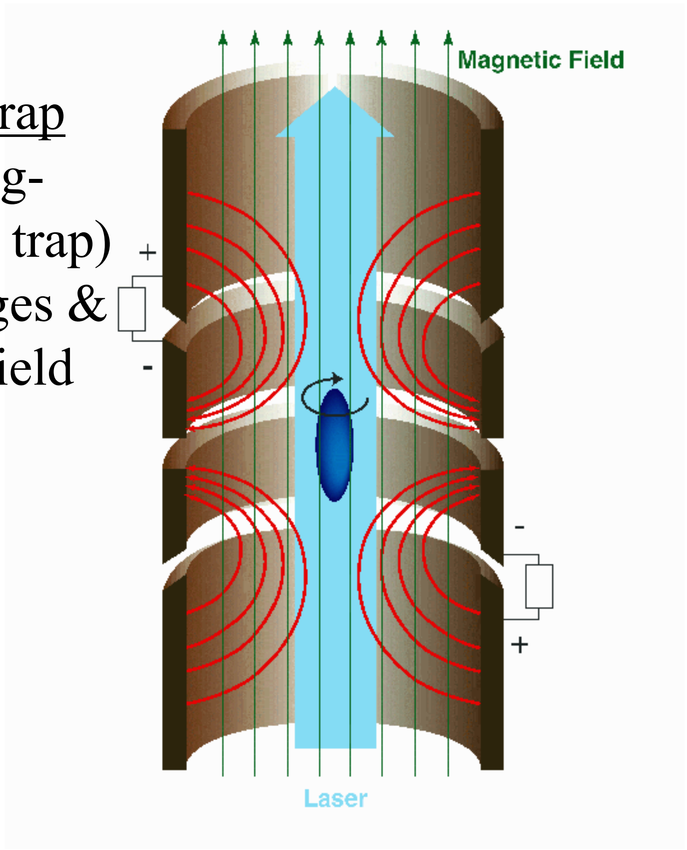

good for laser cooling larger numbers of particles

Penning –Malmberg traps

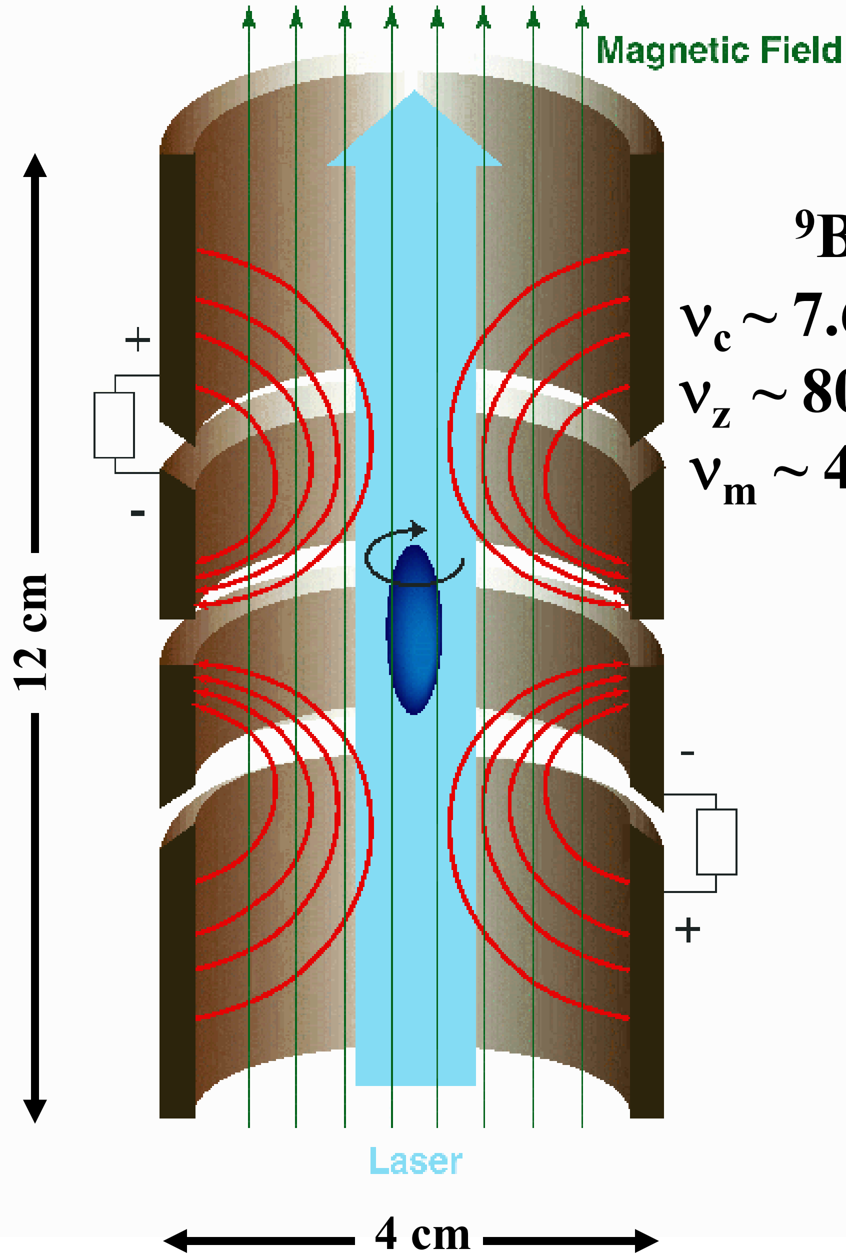

$^9Be^+$

$\nu_c \sim 7.6$ MHz

$\nu_z \sim 800$ kHz

$\nu_m \sim 40$ kHz

g-factors, atomic phys.	–	U of Wash., Mainz, Imperial College, …
mass spectroscopy	–	U of Wash., MIT, Harvard, ISOLDE/CERN, …
cluster studies	–	Mainz/Griefswald
non-neutral plasmas	–	UCSD, Berkeley, Princeton, NIST, …
anti-matter	–	UCSD, Harvard, CERN, Swansea, …

NIST Penning trap

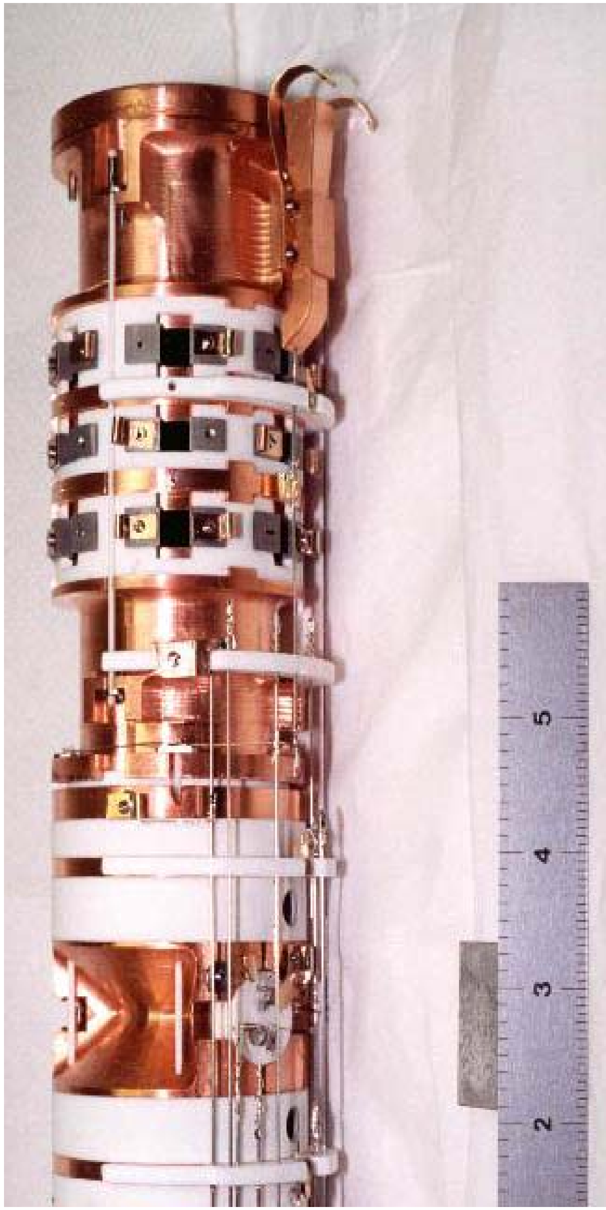

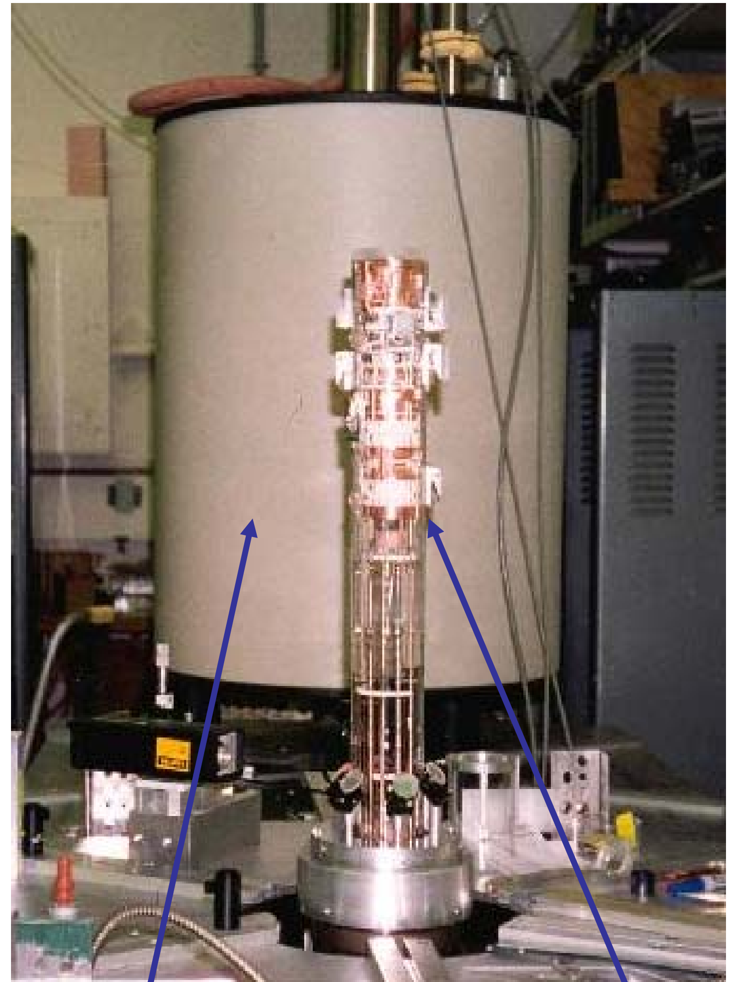

4.5 Tesla
Super Conducting
Solenoid

Quartz
Vacuum envelope
$P < 10^{-10}$ Torr

Non-neutral plasmas in traps evolve into

bounded thermal equilibrium states

thermal equilibrium, Hamiltonian and total canonical angular momentum conserved ⇒

$$f(\mathbf{r},\mathbf{v}) \propto \exp[-(h+\omega_r p_\theta)/k_B T]$$

where $h = \frac{m\mathbf{v}^2}{2} + e\phi(\mathbf{r})$ and $p_\theta = m\mathrm{v}_\theta \mathrm{r} + \frac{eB}{2c}\mathrm{r}^2$

$$f(\mathbf{r},\mathbf{v}) \propto n(\mathrm{r},\mathrm{z}) \exp[-\frac{m}{2k_B T}(\mathbf{v}+\omega_r \mathrm{r}\hat{\theta})^2]$$

density distribution

plasma rotates rigidly at frequency ω_r

$$n(\mathrm{r},\mathrm{z}) \propto \exp\{-\frac{1}{k_B T}[e\phi_p(\mathrm{r},\mathrm{z}) + e\phi_T(\mathrm{r},\mathrm{z}) + m\omega_r(\Omega_c - \omega_r)\frac{r^2}{2}]\}$$

Ω_c = eB/mc = cyclotron frequency

plasma potential

trap potential

Lorentz force potential

centrifugal potential

Lorentz-force potential gives radial confinement !!

Equilibrium plasma properties

- thermal equilibrium $\Rightarrow$ rigid rotation ω_r

- $T \sim 0$ $\Rightarrow$ constant plasma density,
  $n_o = 2\varepsilon_o m\omega_r(\Omega_c - \omega_r)/e^2$,
  Ω_c = cyclotron frequency
  plasma density $\rightarrow$ 0 over a Debye length $\lambda_D = [k_B T/(4\pi n_o e^2)]^{1/2}$

- quadratic trap potential, $e\phi_T \sim m\omega_z^2(z^2 - r^2/2)$ $\Rightarrow$ plasma shape is a spheroid

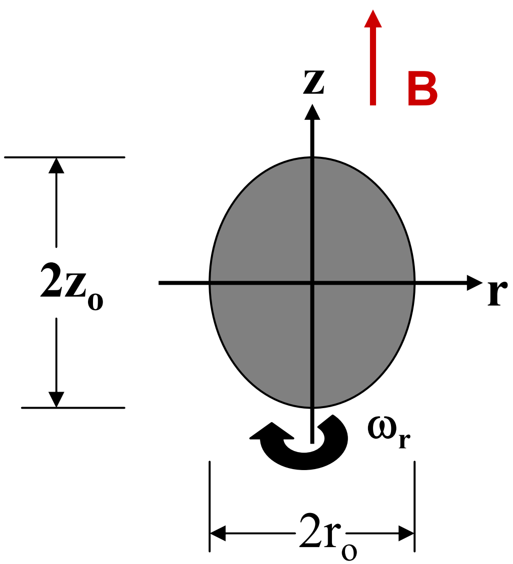

aspect ratio $\alpha \equiv z_o/r_o$
determined by ω_r

$$\frac{\omega_z^2}{2\omega_r(\Omega_c - \omega_r)} = Q_1{}^0\left[\frac{\alpha}{(\alpha^2-1)^{1/2}}\right]/(\alpha^2 - 1)^{1/2}$$

associated Legendre function

Plasma aspect ratio determined by ω_r

$$\frac{\omega_z^2}{2\omega_r(\Omega_c-\omega_r)} = \frac{Q_1{}^0\left[\frac{\alpha}{(\alpha^2-1)^{1/2}}\right]}{(\alpha^2-1)^{1/2}}$$

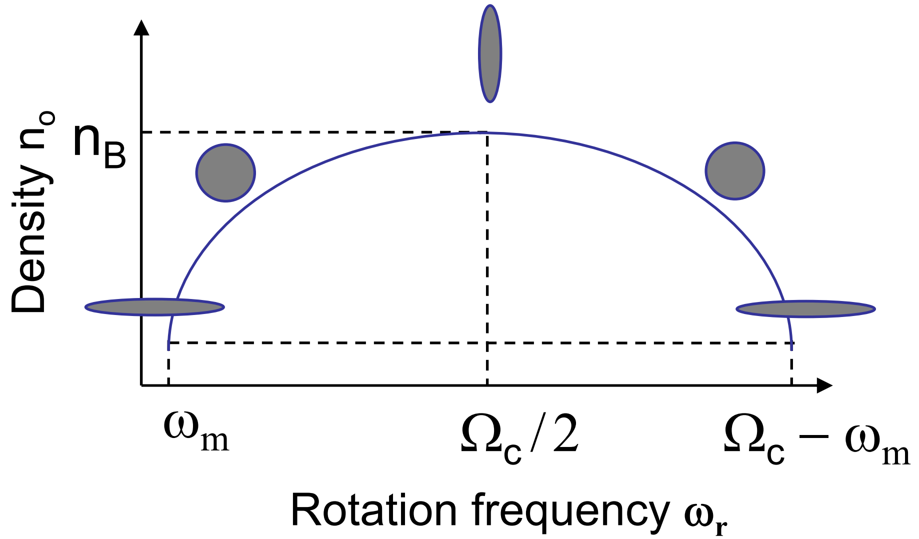

experimental measurements of plasma shape vs ω_r

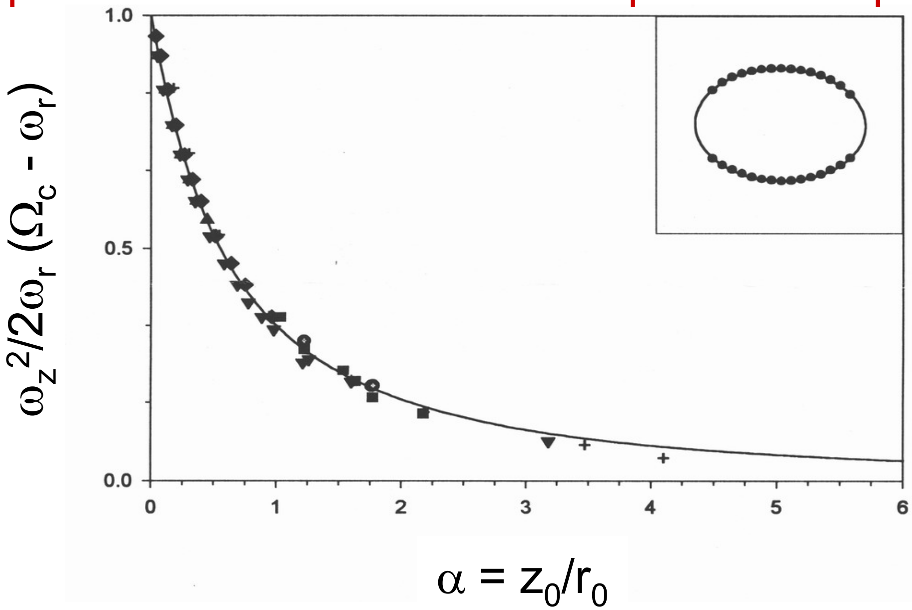

Simple equilibrium theory describes the plasma shapes

Ions in a trap are an example of a one component plasma

- one component plasma (OCP) – consists of a single species of charged particles immersed in a neutralizing background charge

- ions in a trap are an example of an OCP (Malmberg and O'Neil PRL 39, (77))

$$n(\mathrm{r},\mathrm{z}) \propto \exp\{-\frac{1}{k_B T}[e\phi_p(\mathrm{r},\mathrm{z}) + e\phi_T(\mathrm{r},\mathrm{z}) + m\omega_r(\Omega_c - \omega_r)\frac{r^2}{2}]\}$$

looks like neutralizing background

$$\nabla^2\{\phi_T(\mathrm{r},\mathrm{z}) + \frac{1}{e}m\omega_r(\Omega_c - \omega_r)\frac{r^2}{2}\} = -4\pi e n_{bkgnd}$$

$$n_{bkgnd} = -\frac{m\omega_r(\Omega_c - \omega_r)}{2\pi e^2}$$

- thermodynamic state of an OCP determined by:

$$\Gamma \equiv \frac{q^2}{a_{WS} k_B T}, \quad \frac{4}{3}\pi a_{WS}{}^3 n \equiv 1$$

$$\Gamma \approx \frac{\text{potential energy between neighboring ions}}{\text{ion thermal energy}}$$

$\Gamma > 1 \Rightarrow$ **strongly coupled OCP**

Why are strongly coupled OCP's interesting?

- **Strongly coupled OCP's are models of dense astrophysical matter – example: outer crust of a neutron star**

- **For an infinite OCP,** $\Gamma > 2 \Rightarrow$ **liquid behavior**
  $\Gamma \sim 173 \Rightarrow$ **liquid-solid phase transition to bcc lattice**

  Brush, Salin, Teller (1966) $\Gamma \sim 125$
  Hansen (1973) $\Gamma \sim 155$
  Slatterly, Doolen, DeWitt(1980) $\Gamma \sim 168$
  Ichimaru; DeWitt; Dubin (87-93) $\Gamma \sim 172\text{-}174$

- **Coulomb energies/ion of bulk bcc, fcc, and hcp lattices differ by** $< 10^{-4}$

body centered cubic

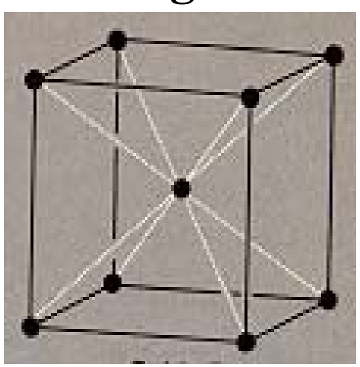

face centered cubic

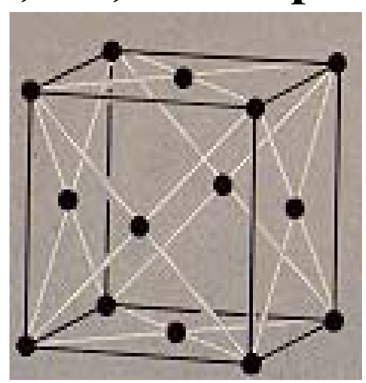

hexagonal close packed

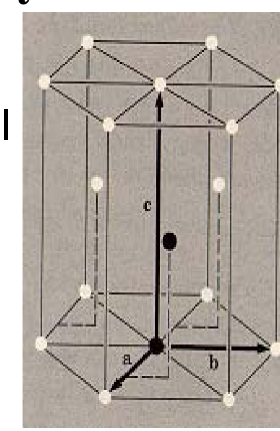

- **with trapped ions,** $n_o \sim 10^9\ \text{cm}^{-3}$
  $T < 5\ \text{mK}$ $\Rightarrow$ $\Gamma > 500$

Plasmas vs strongly coupled plasmas

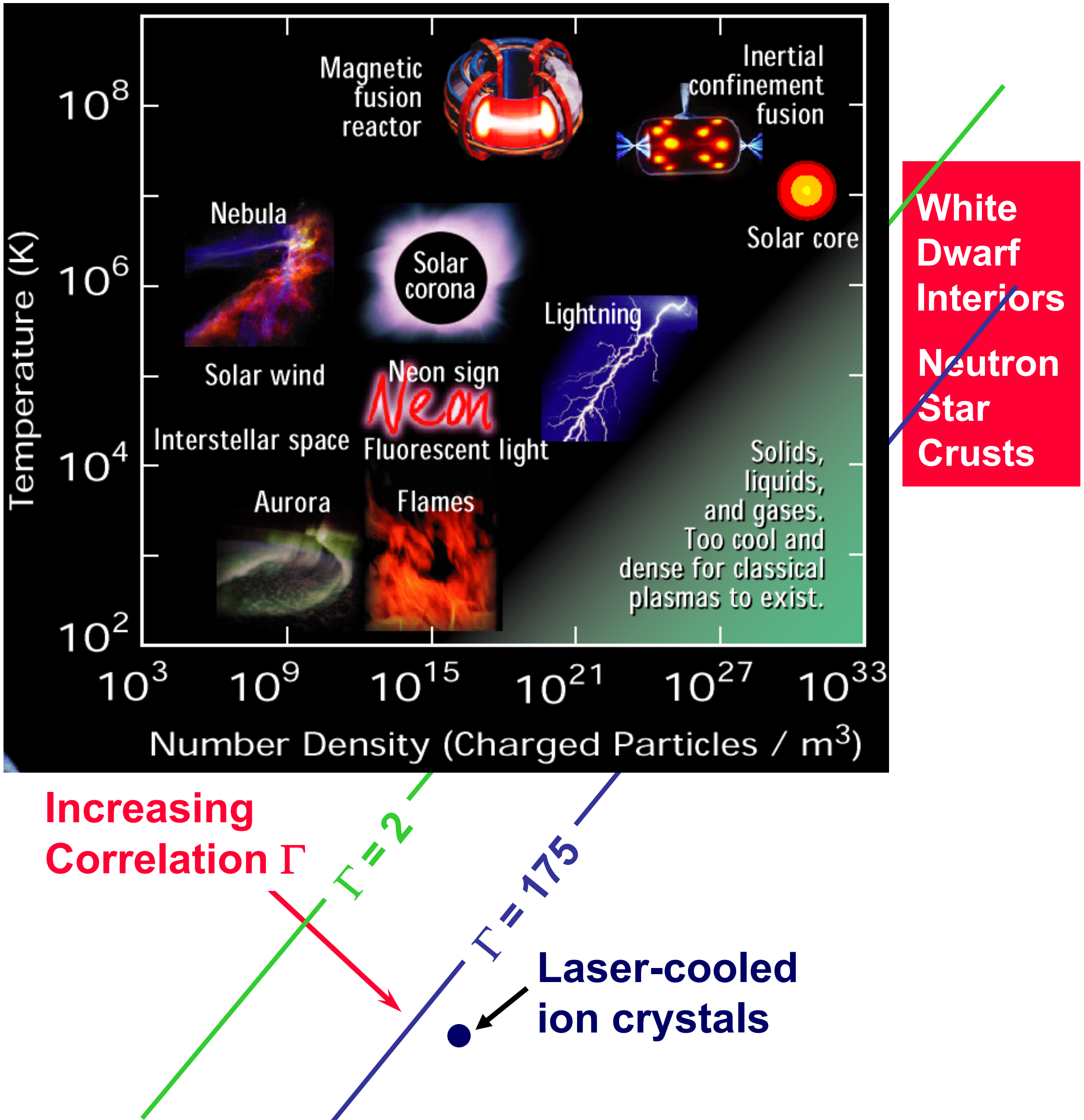

Are there other laboratory strongly coupled OCP's?

- rf traps - Drewsen (Aarhus) – rf micromotion limits plasma size
- ion storage rings $T_{||} \sim$ few mK$\rightarrow$K, $T_{\perp} >> T_{||}$
  - ion strings observed in GSI (200 MeV/μ, fully stripped ions)
  - 1 eV ion crystals observed in PALLAS (Schramm, Nature 2001)
- ultra-cold neutral plasmas $n \geq 10^9$ cm^{-3}, T~10 μK before photo-ionization

  Rolston (NIST); Raithel (Mich.); Killian (Rice); Eyler/Gould (UConn); Bergerson (BYU); Gallagher (UVA); …

other strongly coupled (screened) Coulomb systems

- dusty plasma crystals

  Melzer, *et al*., PRE 53, 2757 (96)
  Thomas *et al*., Nature 379, 806 (96)
  Pieper, *et al*., PRE 54, 5636 (96)

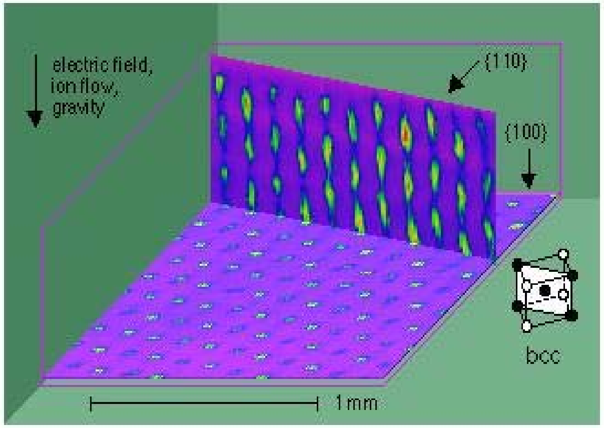

3-d dusty plasma crystal; from Goree, U. of Iowa

- colloidal suspensions

  Murray & Grier, American Scientist **83**, 238 (95)
  Vos *et al*., Langmuir **13**, 6004 (97)

Strongly coupled plasma work in ion traps

- 1987 – Coulomb clusters in Paul traps
  MPI Garching (Walther)
  NIST (Wineland)

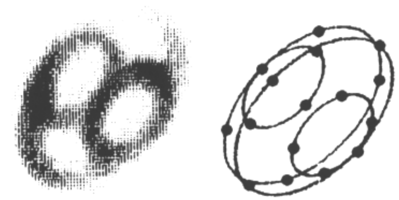

- 1988 – shell structures in Penning traps
  NIST group

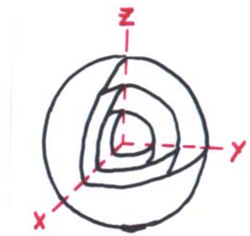

- 1992 – 1-D periodic crystals in linear Paul traps
  MPI Garching

  Nature 357, 310 (92)

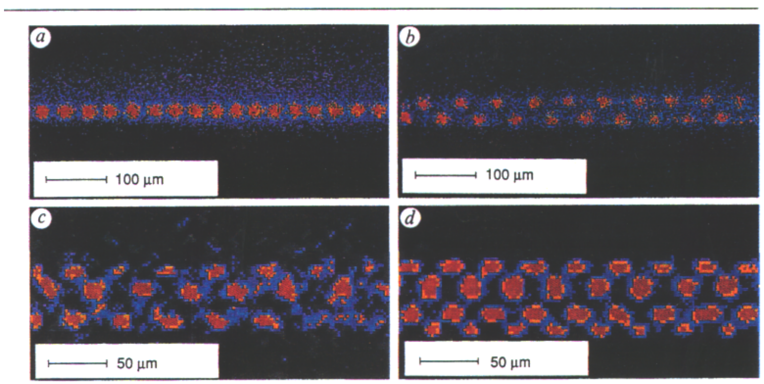

- 1998 – 1-D periodic crystals with plasma diameter
  $> 30\ a_{WS}$
  Aarhus group

  PRL 81, 2878 (98)

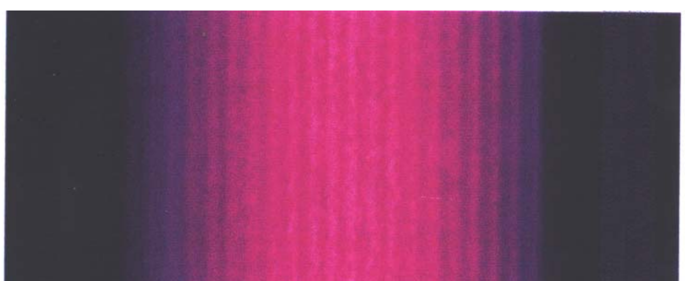

How large must a plasma be to exhibit a bcc lattice?

1989 - Dubin, planar model PRA 40, 1140 (89)

result: plasma dimensions ≥ 60 interparticle spacings required for bulk behavior

$N > 10^5$ in a spherical plasma ⇒ bcc lattice

2001 – Totsji, simulations, spherical plasmas, N≤120 k

PRL 88, 125002 (2002)

result: N>15 k in a spherical plasma ⇒ bcc lattice

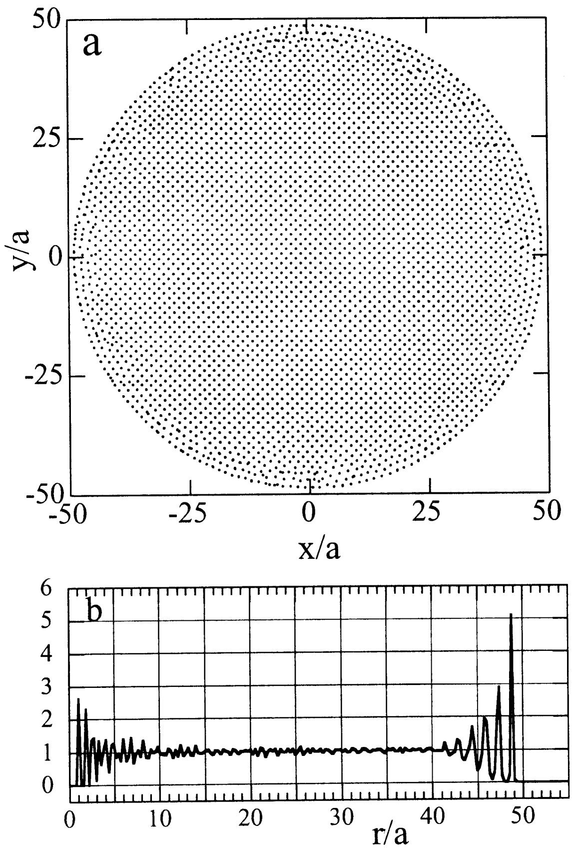

Doppler laser cooling

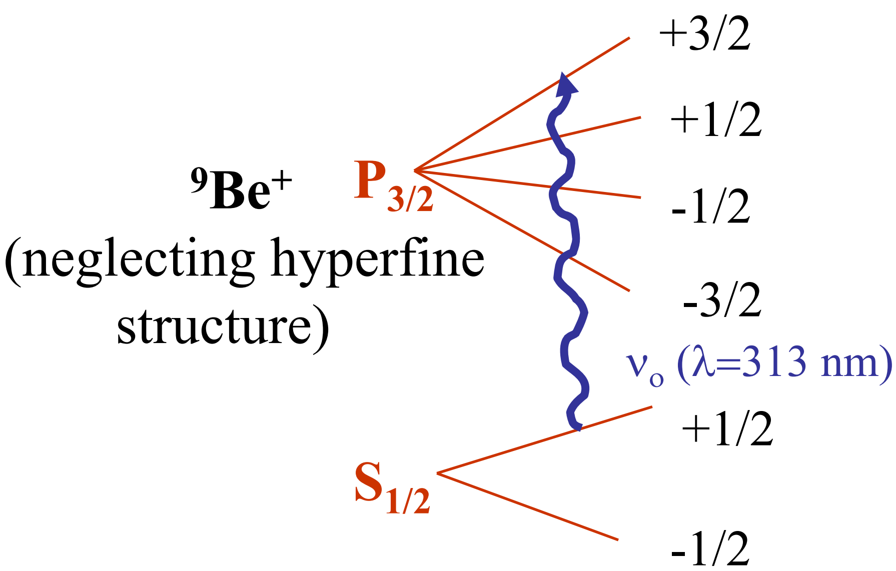

$T_{min}(^9Be^+) \sim 0.5$ mK

$T_{measured} < 1$ mK

Laser torque

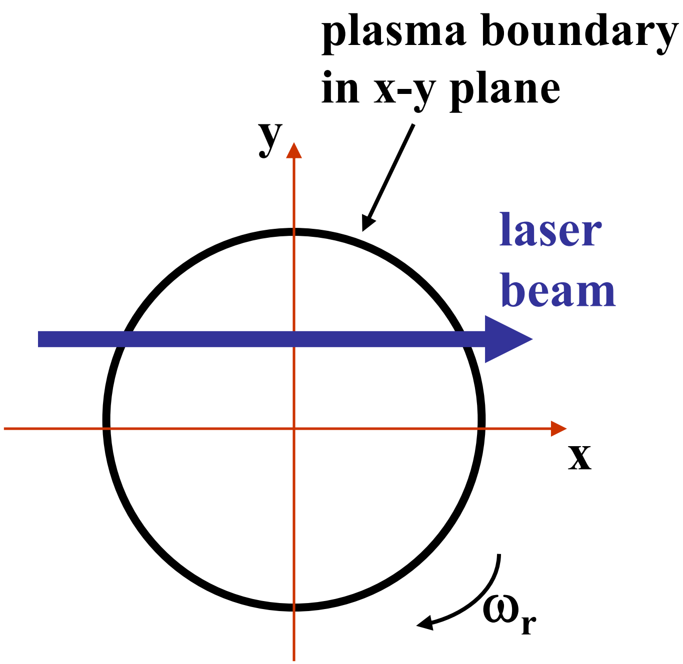

The laser beam position and frequency control the torque and ω_r

With the laser beam directed as shown, increasing torque $\Rightarrow$ increasing ω_r $\Rightarrow$ decreasing radius

NIST Bragg scattering set-up

$f_{rotation}$ = 240 kHz
n = 7.2 x 10^8 /cm^3

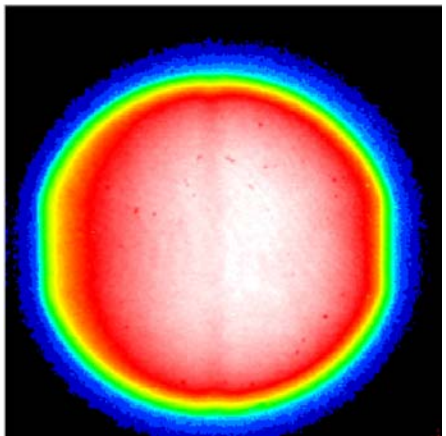

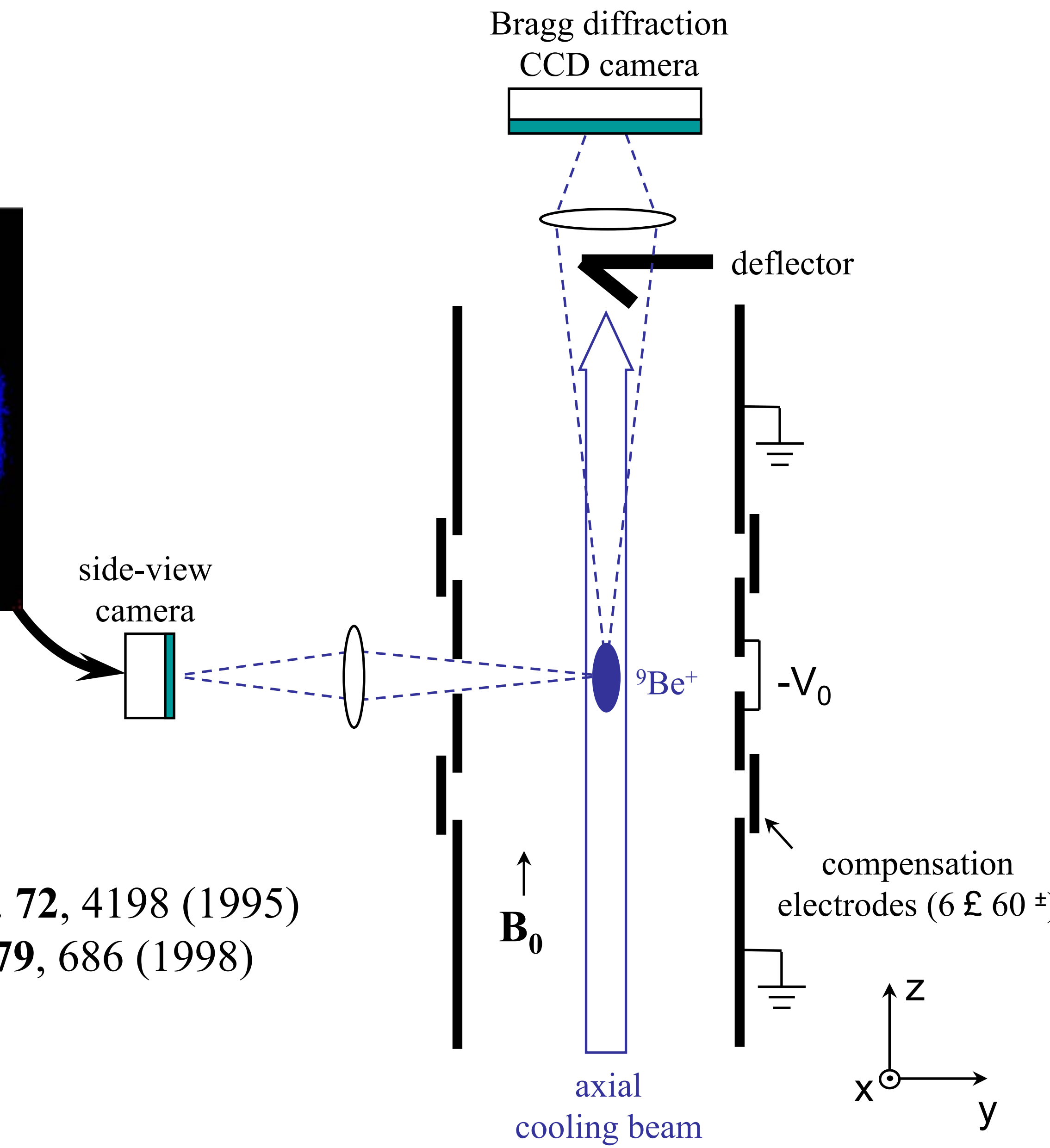

J.N. Tan, *et al.*, Phys. Rev. Lett. **72**, 4198 (1995)
W.M. Itano, *et al.*, Science **279**, 686 (1998)

Bragg scattering from spherical plasmas with N~ 270 k ions

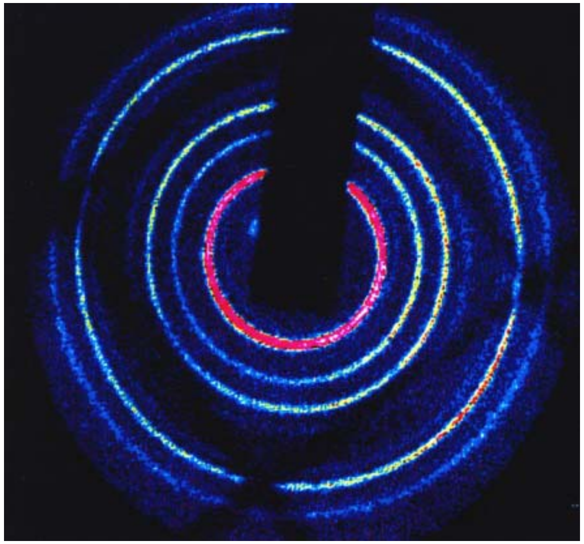

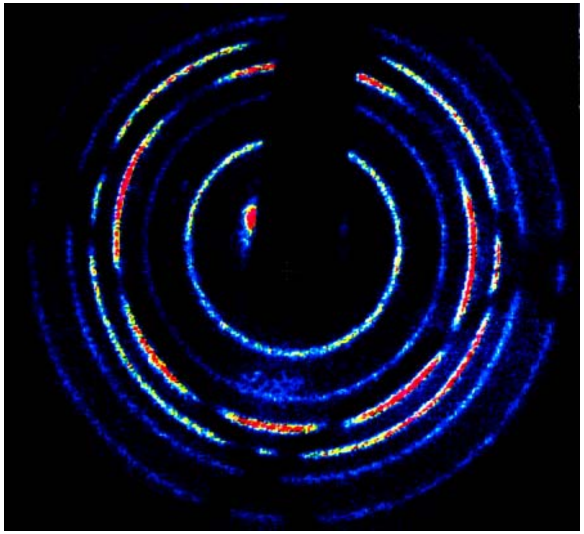

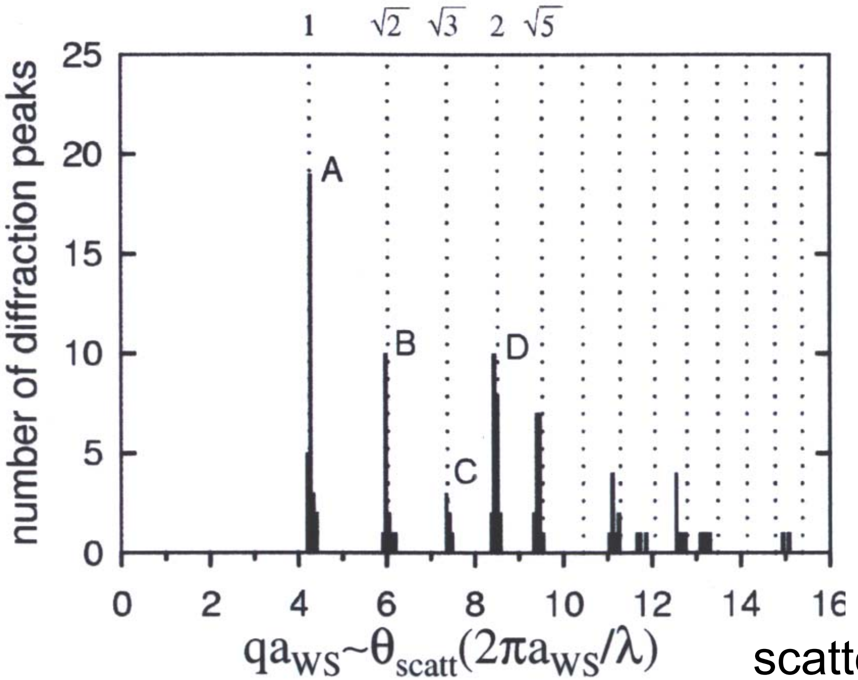

scattering angle →

Evidence for bcc crystals

Rotating wall control of the plasma rotation frequency

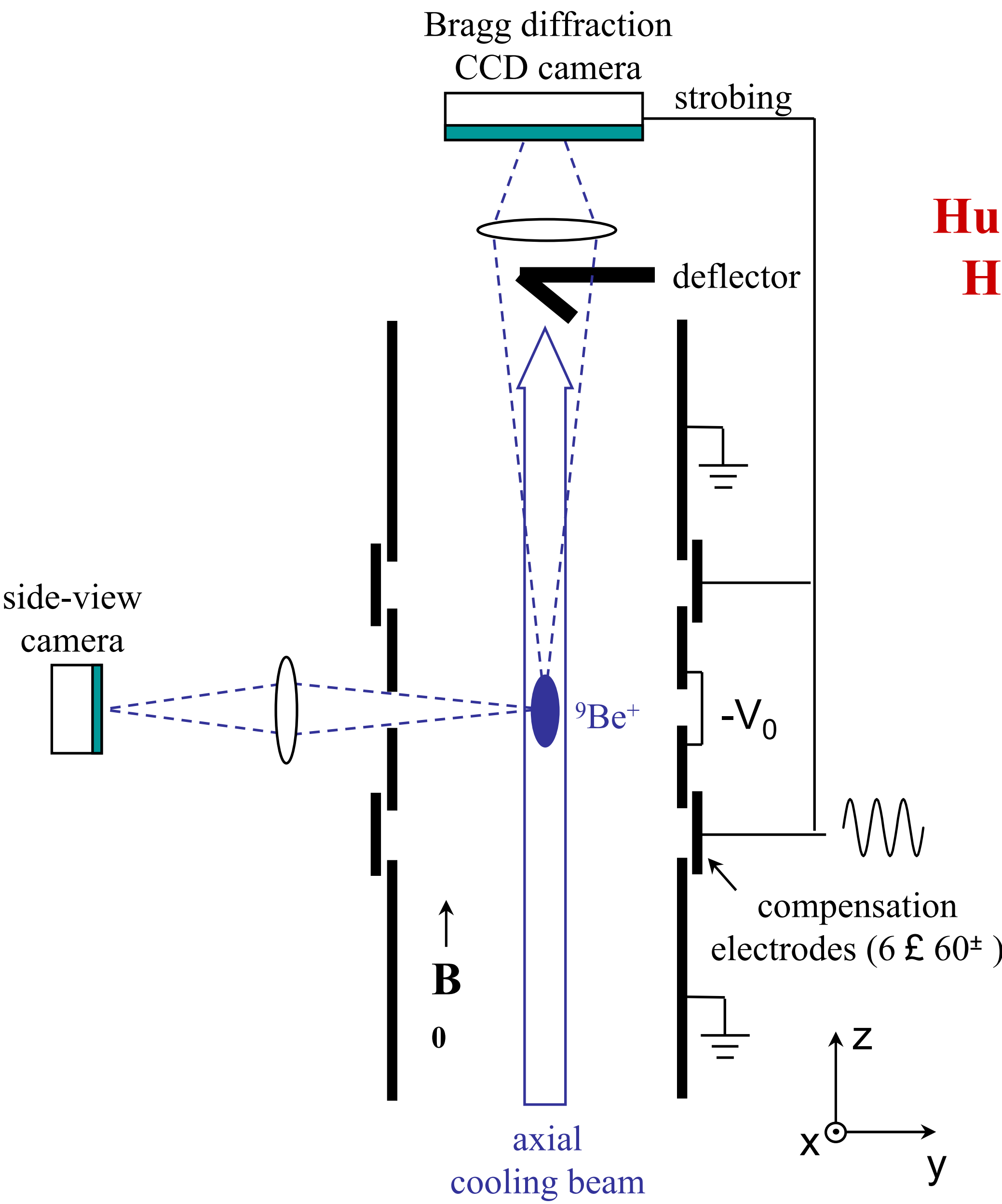

Huang, *et al.* (UCSD), PRL 78, 875 (97)
Huang, *et al.* (NIST), PRL 80, 73 (98)

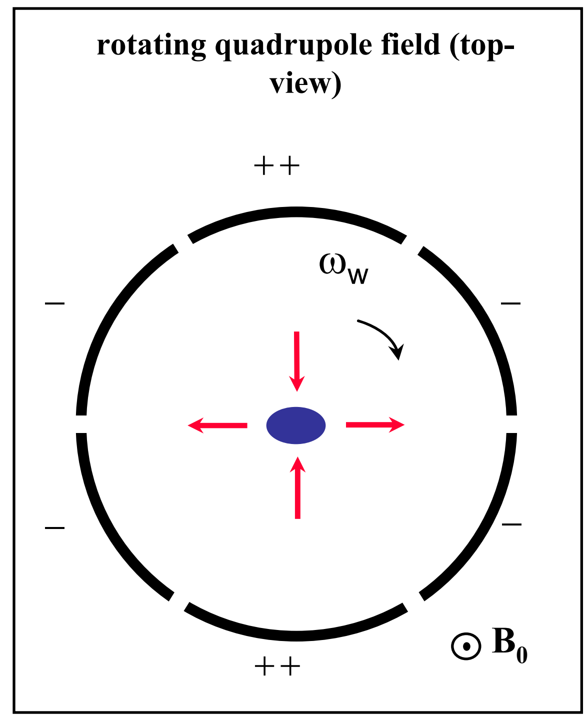

Phase-locked control of the plasma rotation frequency

Huang, *et al.*, Phys. Rev. Lett. 80, 73 (98)

time averaged Bragg scattering

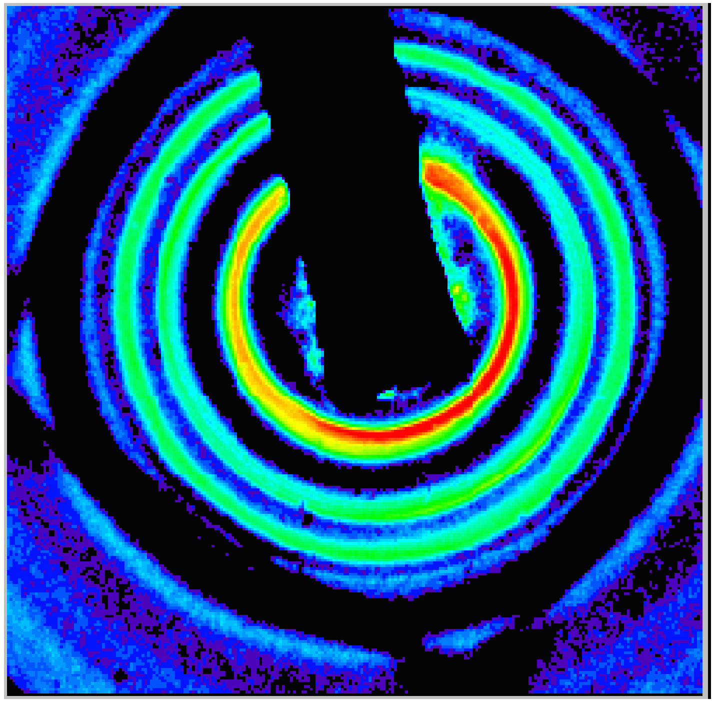

camera strobed by the rotating wall

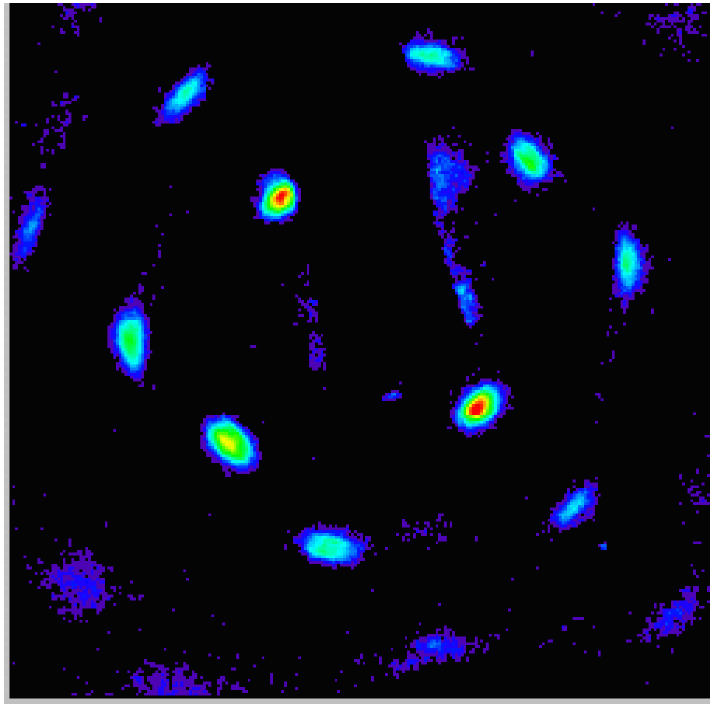

- **N > 200,000 ions ⇒ always observe bcc crystalline patterns**
- **100,000> N > 20,000 ⇒ observe fcc, hcp?, in addition to bcc**

Real space imaging

Mitchell. *et al.*, Science **282**, 1290 (98)

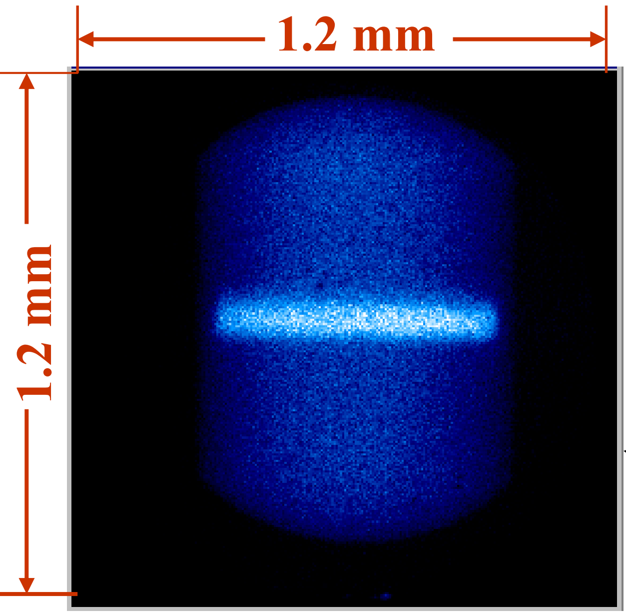

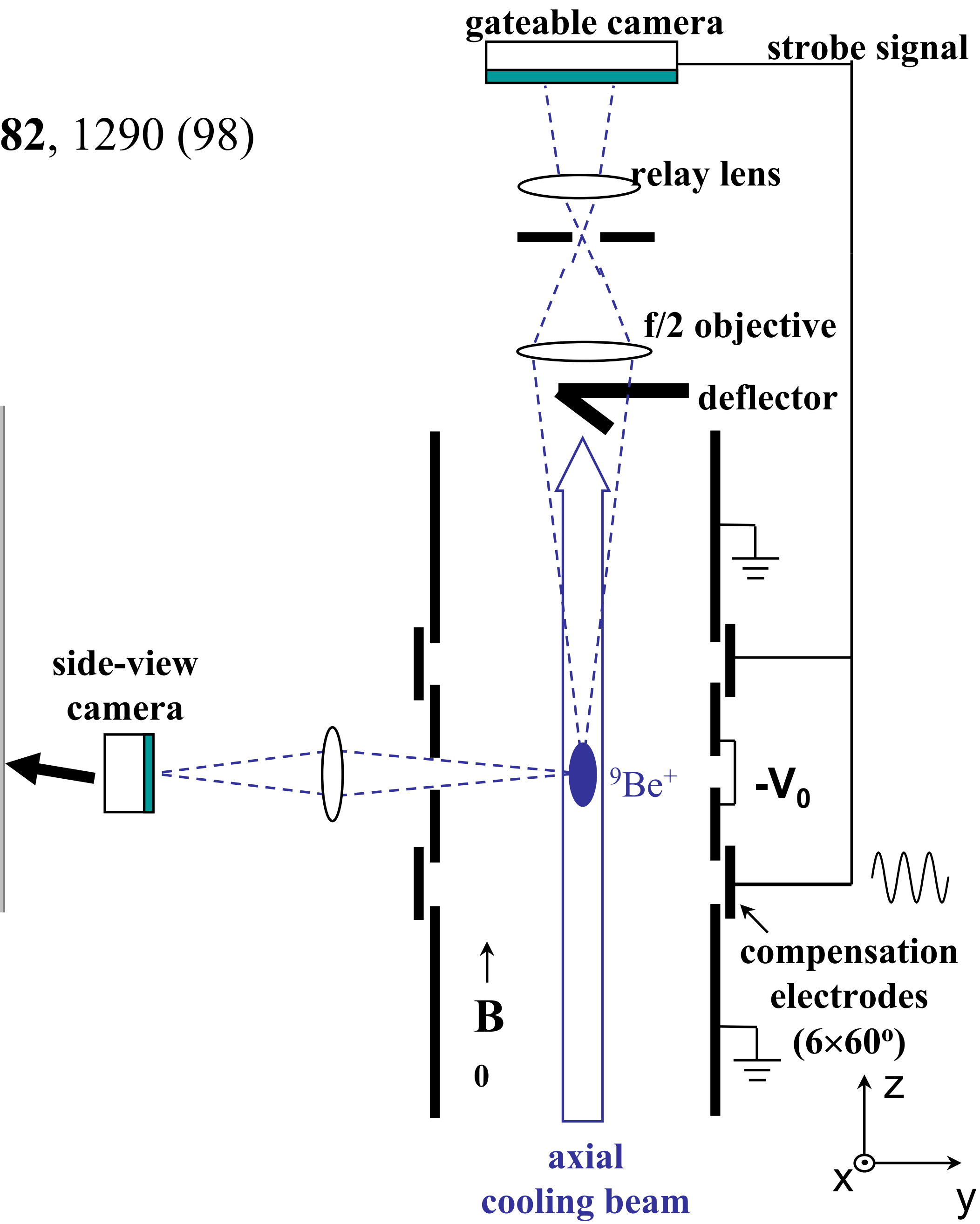

Top-view images in a spherical plasma of ~180,000 ions

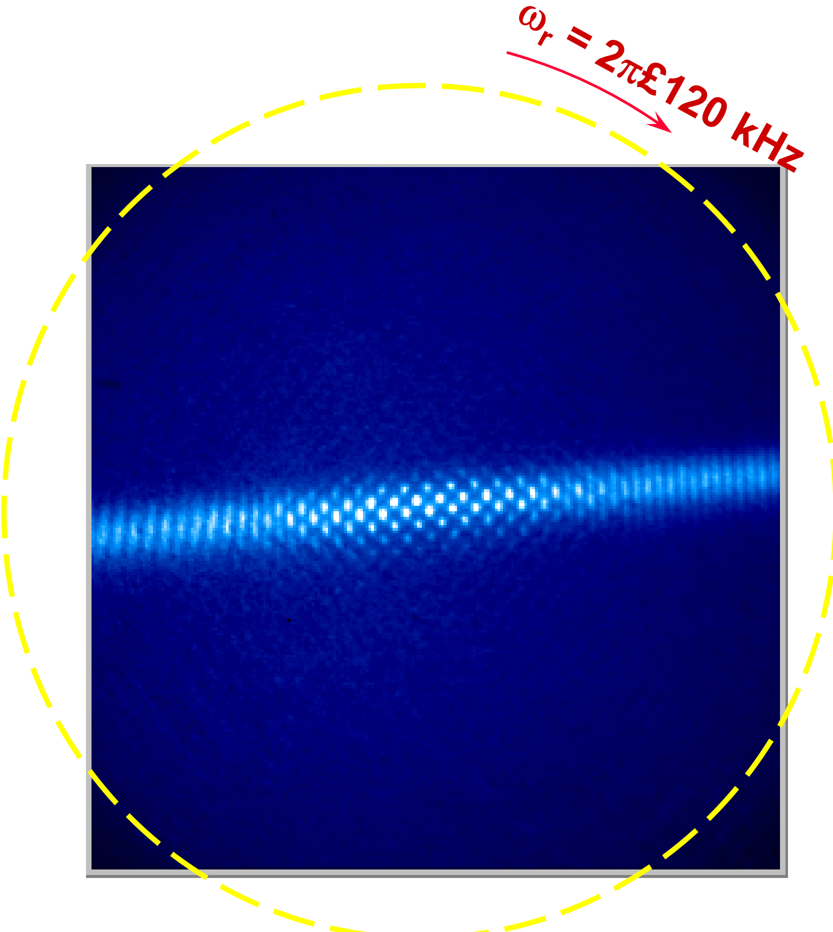

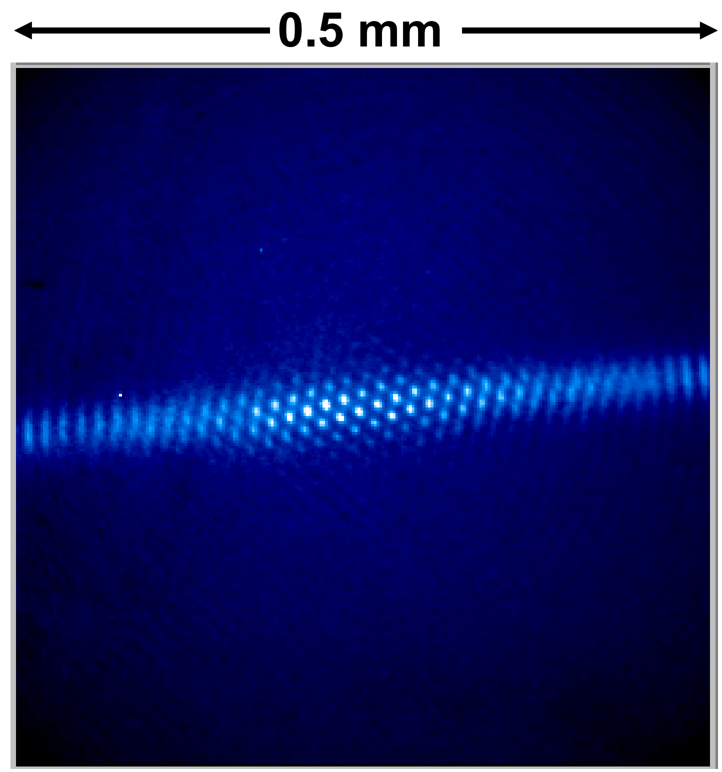

bcc (100) plane

predicted spacing: 12.5 μm

measured: 12.8 ± 0.3 μm

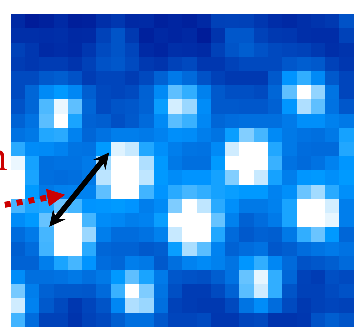

bcc (111) plane

predicted spacing: 14.4 μm

measured: 14.6 ± 0.3 μm

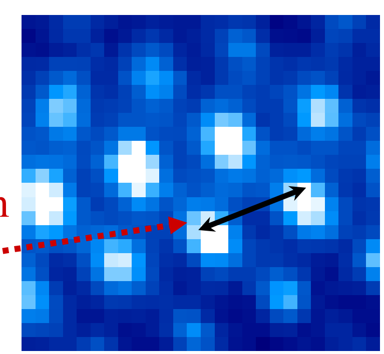

Real-space images with planar plasmas

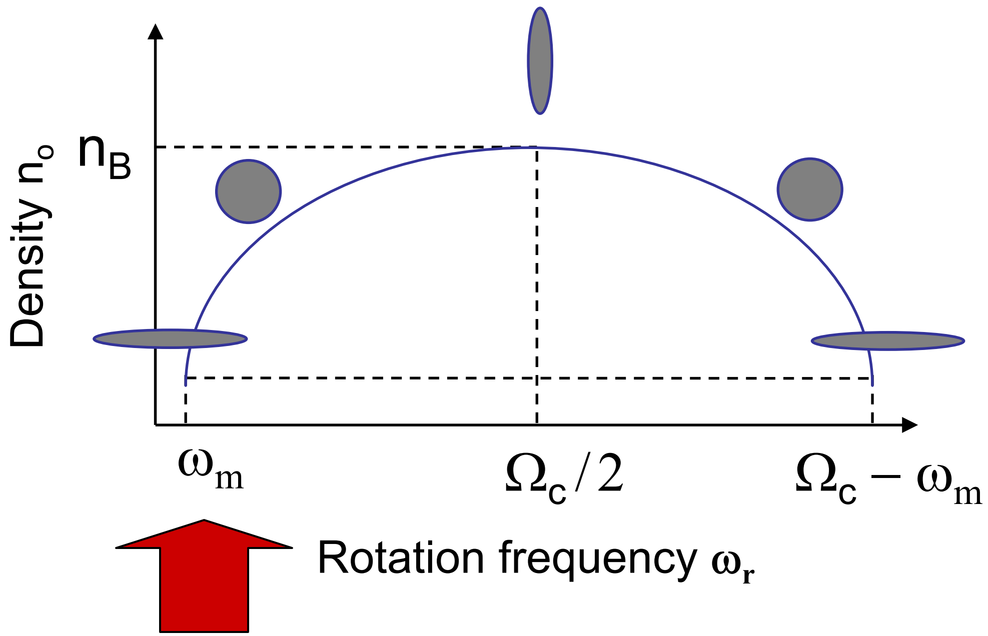

with planar plasmas all the ions can reside within the depth of focus

Planar structural phases can be 'tuned' by changing ω_r

top-views

65.70 kHz

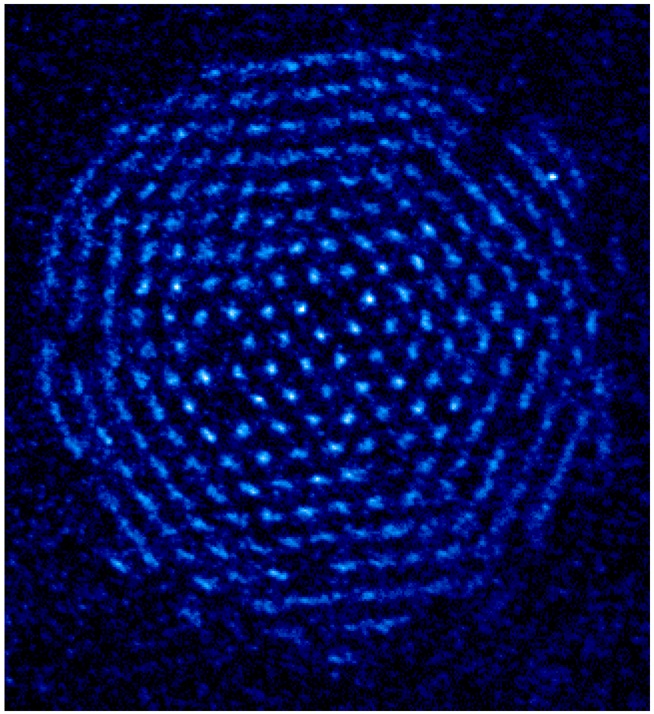

66.50 kHz

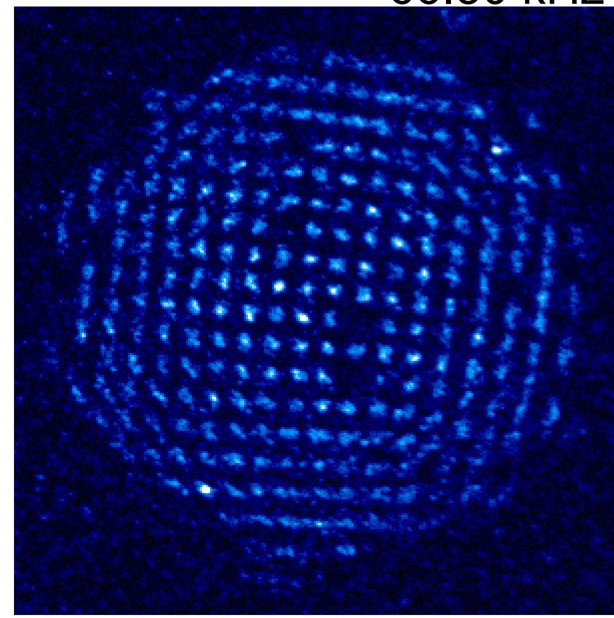

side-views

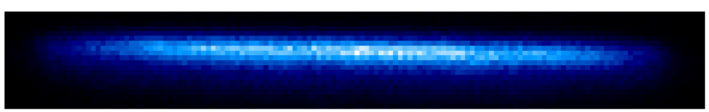

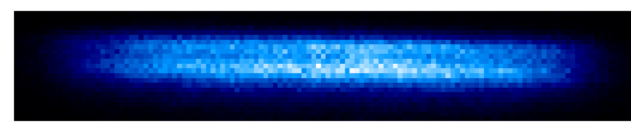

1 lattice plane, hexagonal order

2 planes, cubic order

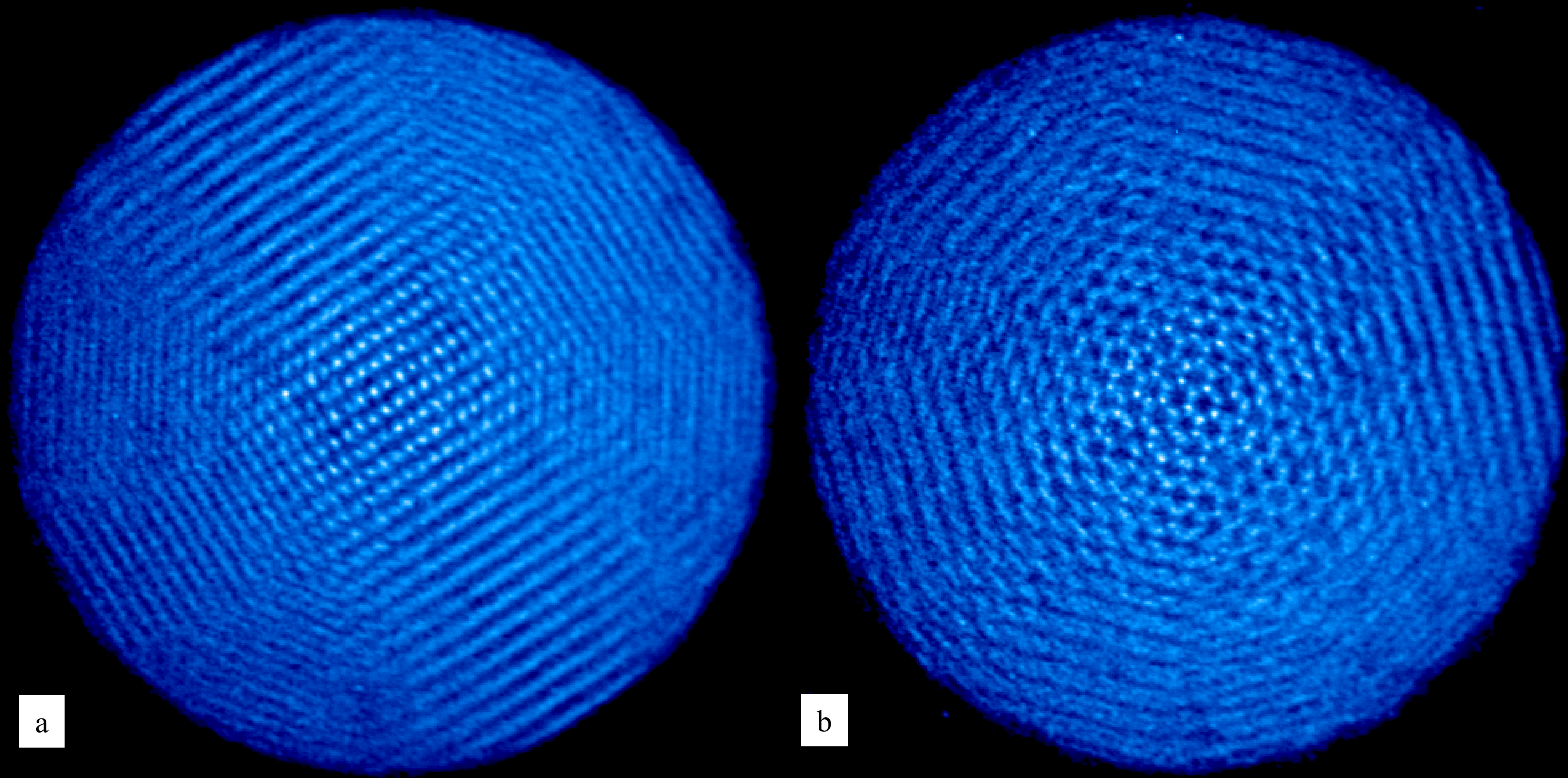

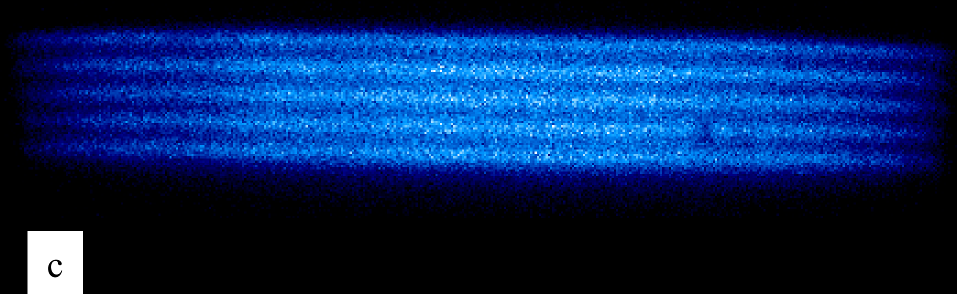

Top- (a,b) and side-view (c) images of crystallized $^{9}Be^{+}$ ions contained in a Penning trap. The energetically favored phase structure can be selected by changing the density or shape of the ion plasma. Examples of the (a) staggered rhombic and (b) hexagonal close packed phases are shown.

Mitchell, *et al.*, Science **282**, 1290 (98)

Theoretical curve from Dan Dubin, UCSD

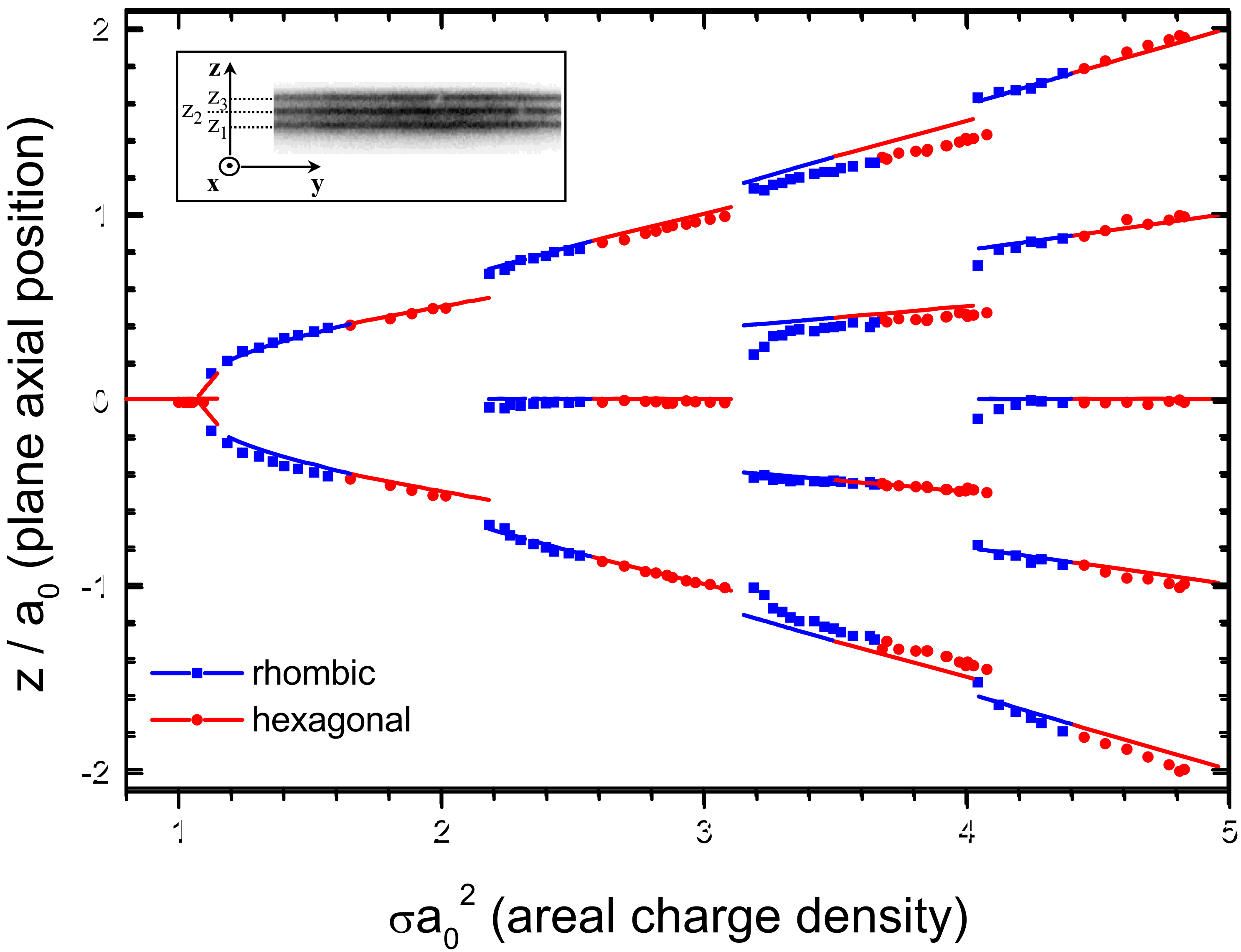

increasing rotation frequency →

Stick-slip motion of the crystal rotation

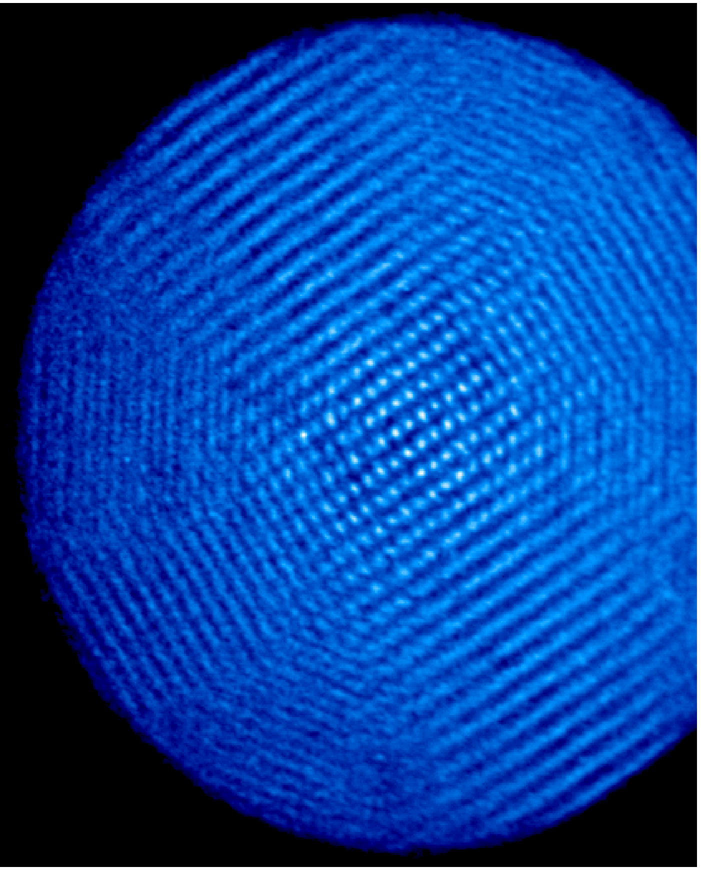

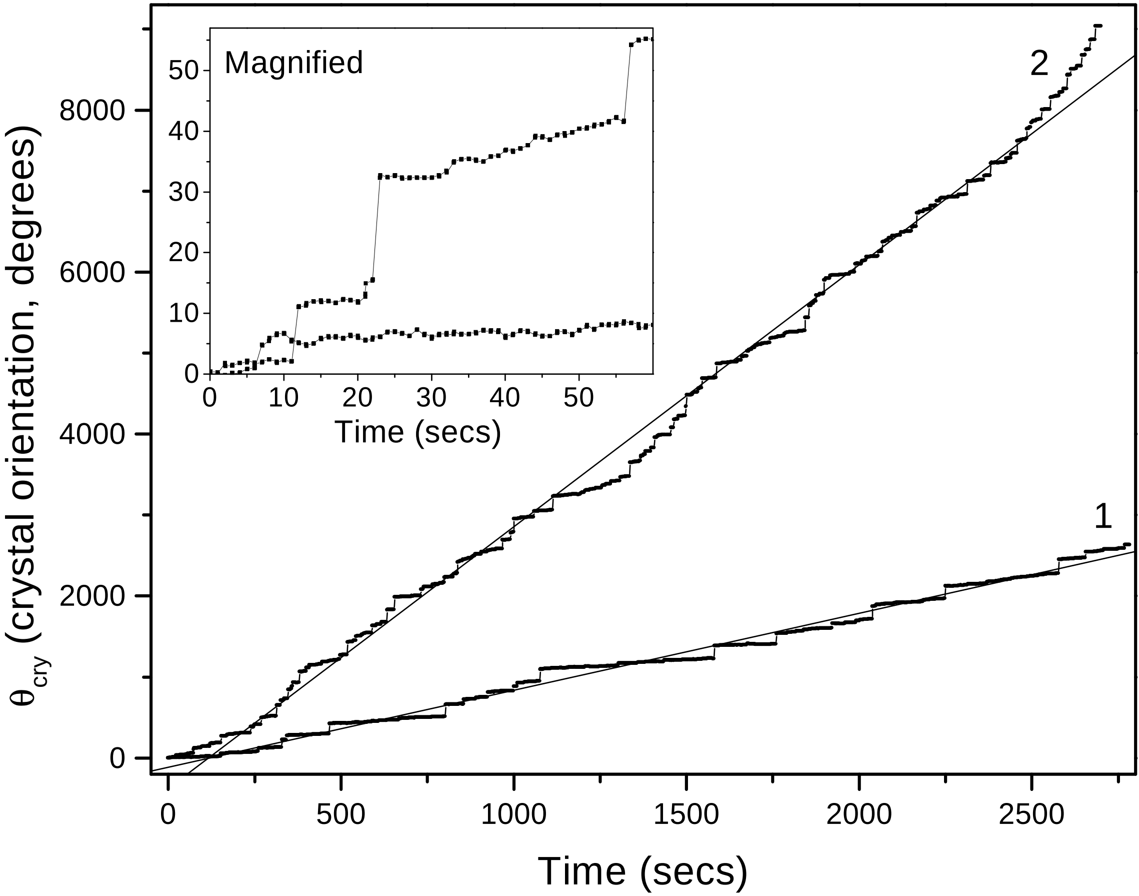

- **not a true phase lock!**
- **frequency offset (ω_r-ω_{wall}) due to creep of 2 -18 mHz**
- **regions of phase-locked separated by sudden slips in the crystal orientation**
- **stick-slip motion due to competition between ? laser and rotating wall torques**
- **mean time between slips ~10 s; what triggers the slips?**

Summary of crystal observations

spherical plasmas

- **bcc crystals observed with N > 200 k ions**
- **other crystal types (fcc, hcp) observed for 20 k < N <200 k**
- **shell structure observed for N < 20 k ions**

planar plasmas

- **structural phase transitions between rhombic planes (bcc-like) and hexagonal planes (fcc-like or bcc-like)**
- **good agreement with the predicted T=0 minimum energy lattice for plasmas < 10 lattice planes thick**

Can we observe the predicted thermodynamic phase transition at Γ~172?

Phase transition can be determined from the specific heat

- **details of specific heat at the phase transition appear to only weakly depend on N and the type of structure.** **Schiffer, PRL 88, 205003 (2002)**

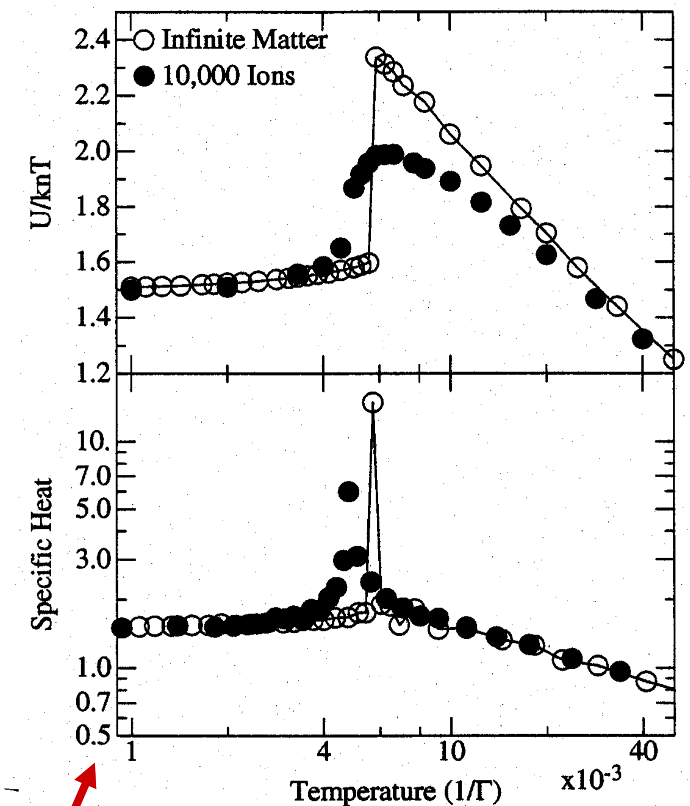

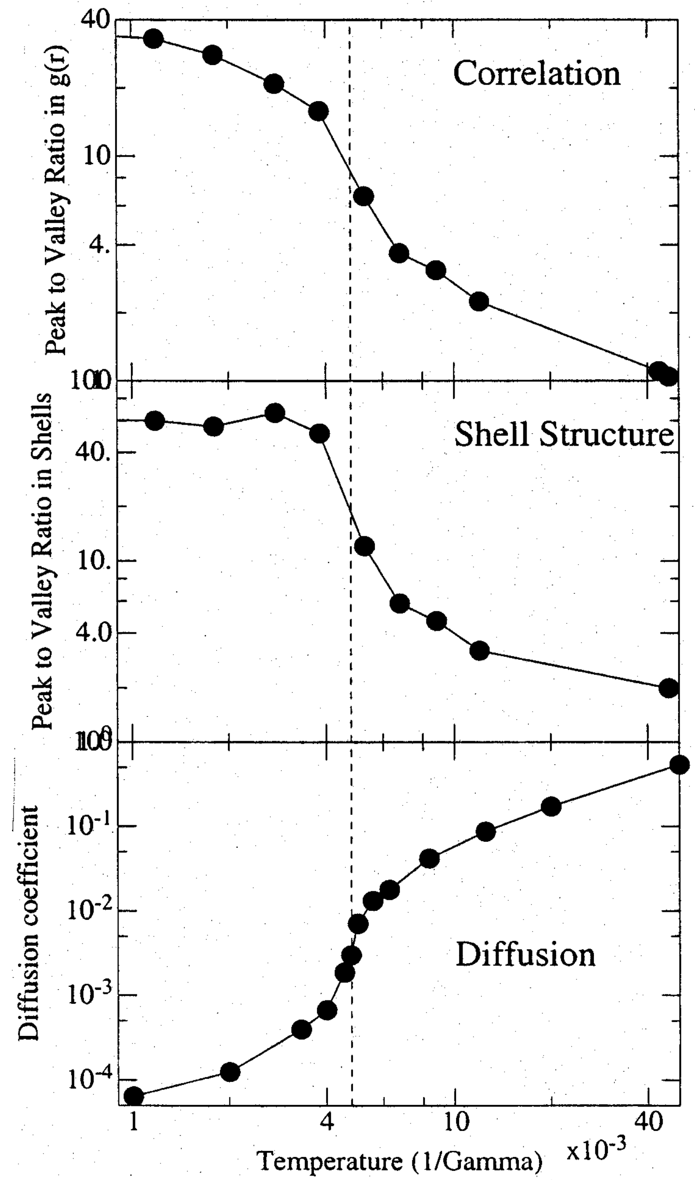

molecular dynamics simulation with a spherical plasma with 10 000 ions in shells

Measure specific heat with a constant (or known) dE/dt

- our dominant heating rate appears to be due to background collisions
  ⇒ constant energy input dE/dt to the plasma, independent of liquid or solid state

- For a sufficiently large plasma where surface effects can be neglected, $E_R = E_R^{(0)} + U$
  where E_R = energy of the plasma in the rotating frame
  $E_R^{(0)}$ = zero-temperature mean-field plasma energy (no correlations, fluid description depends only on ω_r and trap parameters)
  $U = 3NkT/2 + U_{corr}$ = energy of infinite OCP

- Assume constant ω_r , $dE/dt = (3*k*0.1\ K/s)/2$, theoretical expression for U

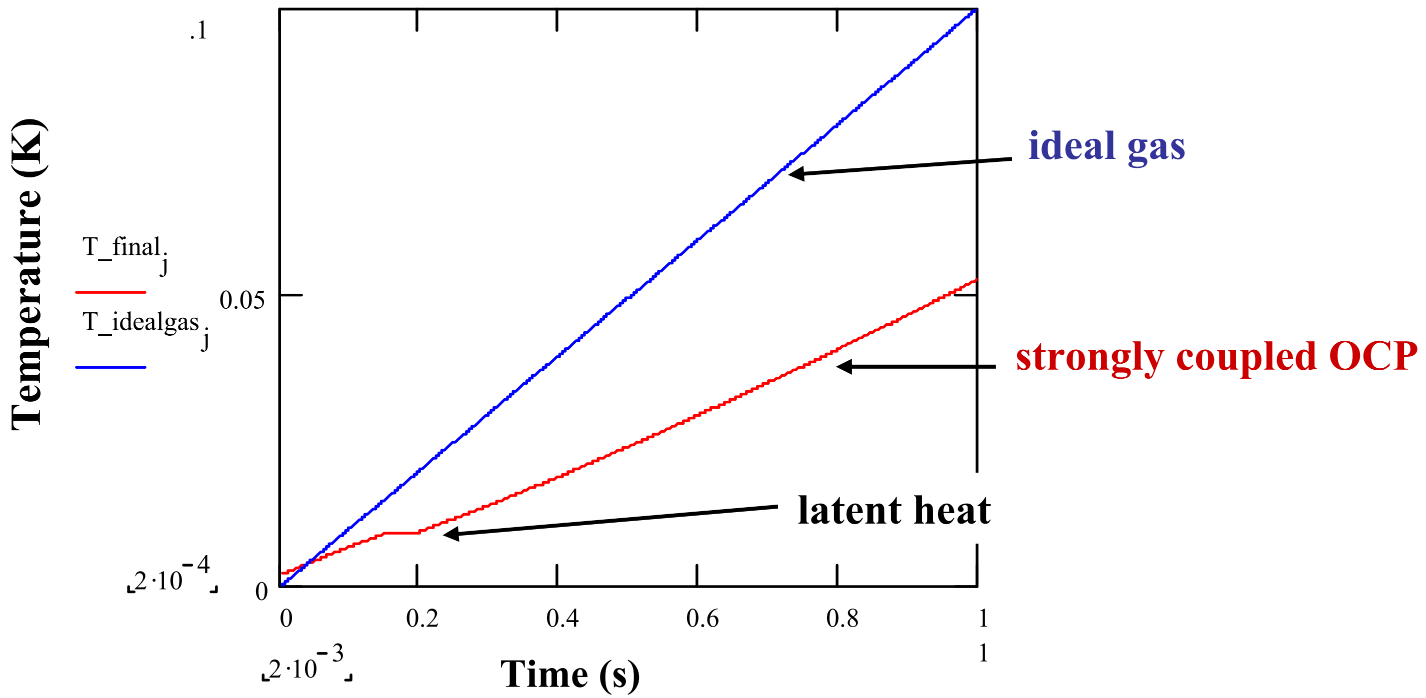

Energy level diagram for $^9Be^+$ in high magnetic field

B high ⇒ (m_I,m_J) basis

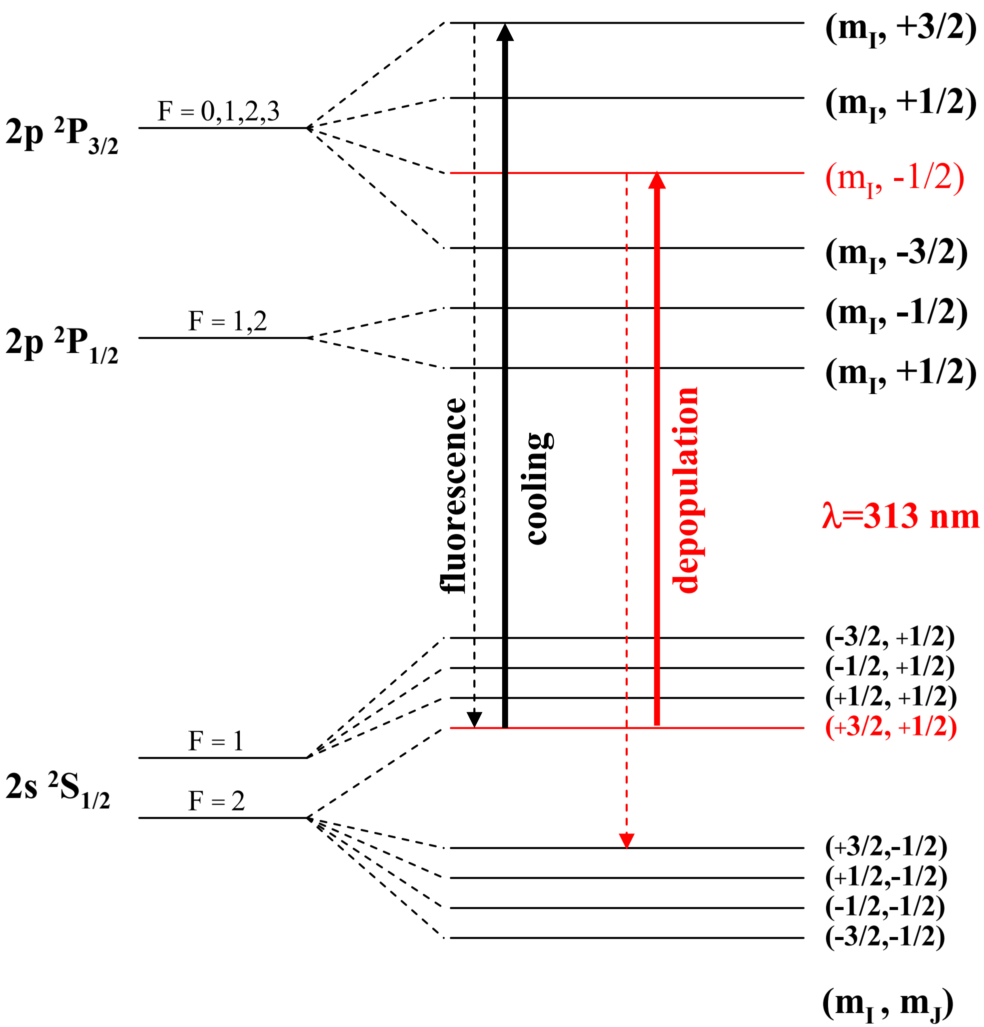

Temperature measurement

- Monitor cooling laser fluorescence
- Depopulation laser resonant ⇒ decrease in fluorescence
- Measure Doppler broadening ⇒ T

Measurement of the ion temperature

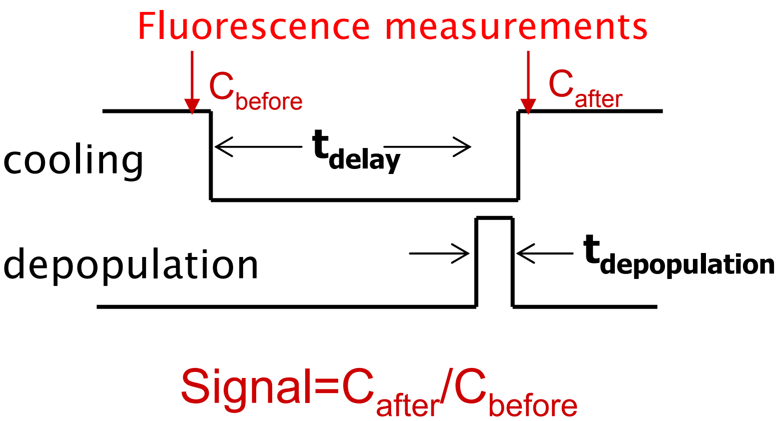

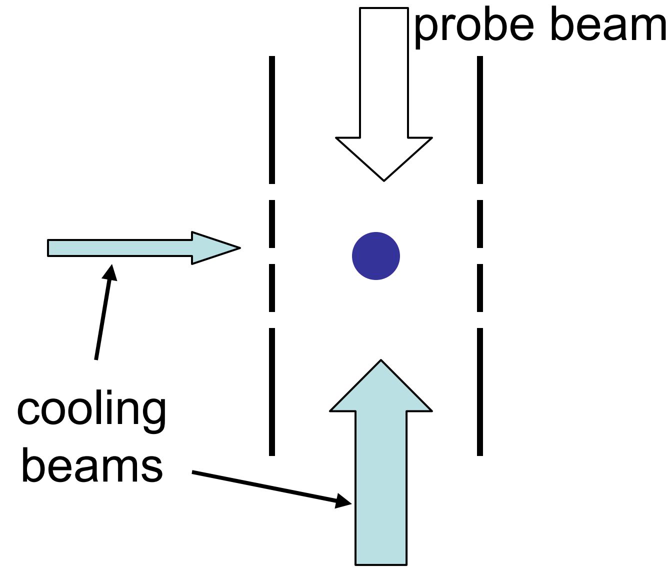

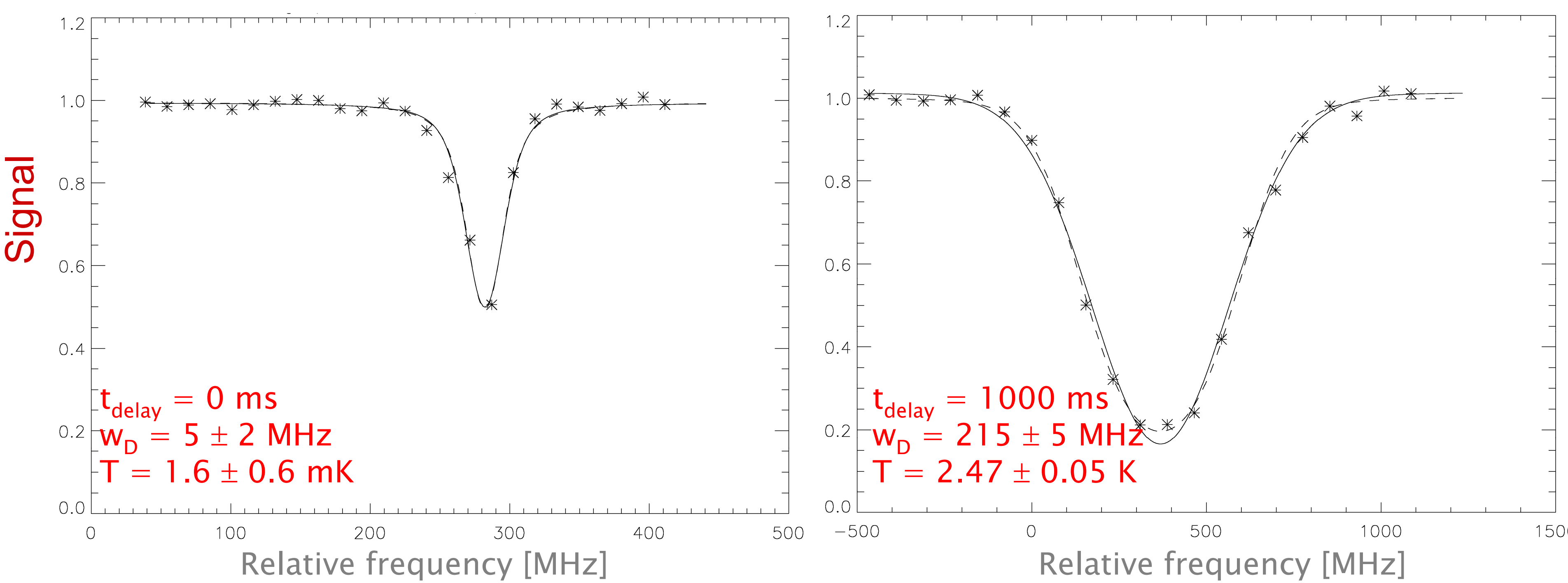

Heating rate measurements

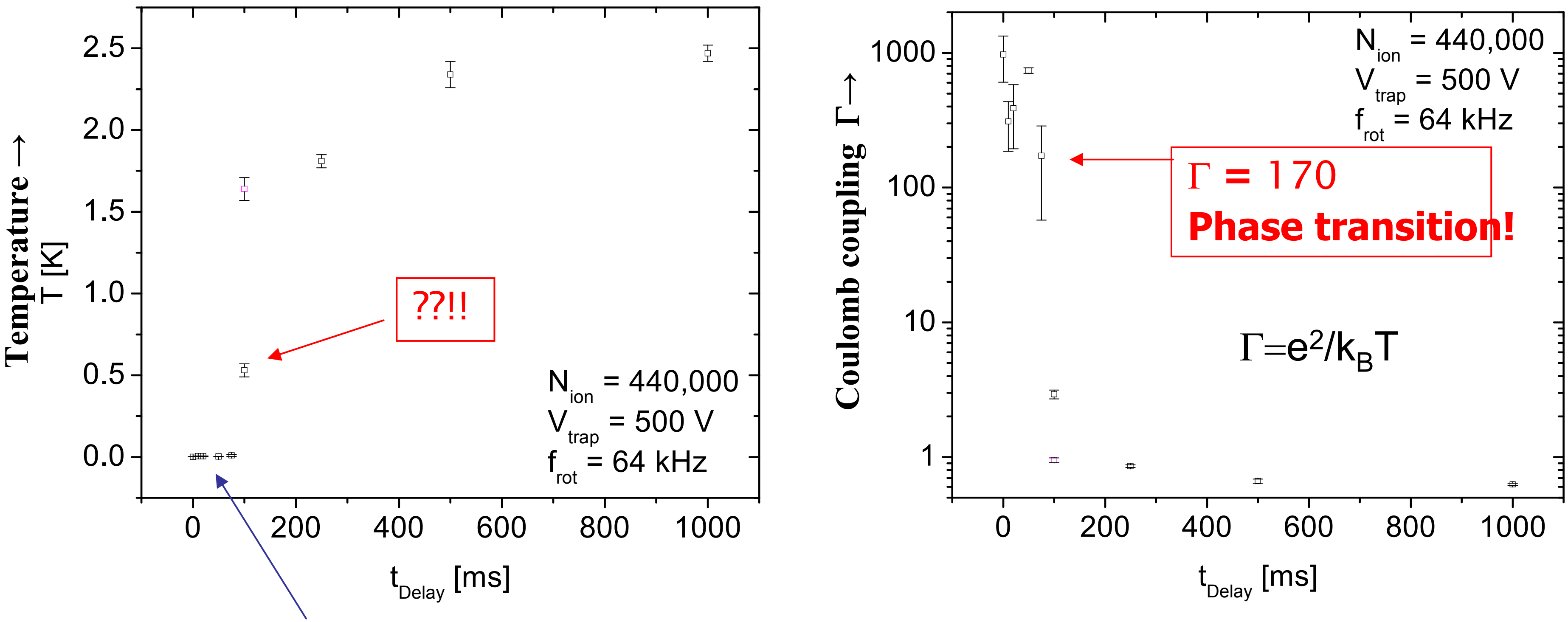

Slow heating at short times: 50-100 mK/s

Miniature RF-traps: ~50 mK/s

More heating curves

Many heating rate curves later…

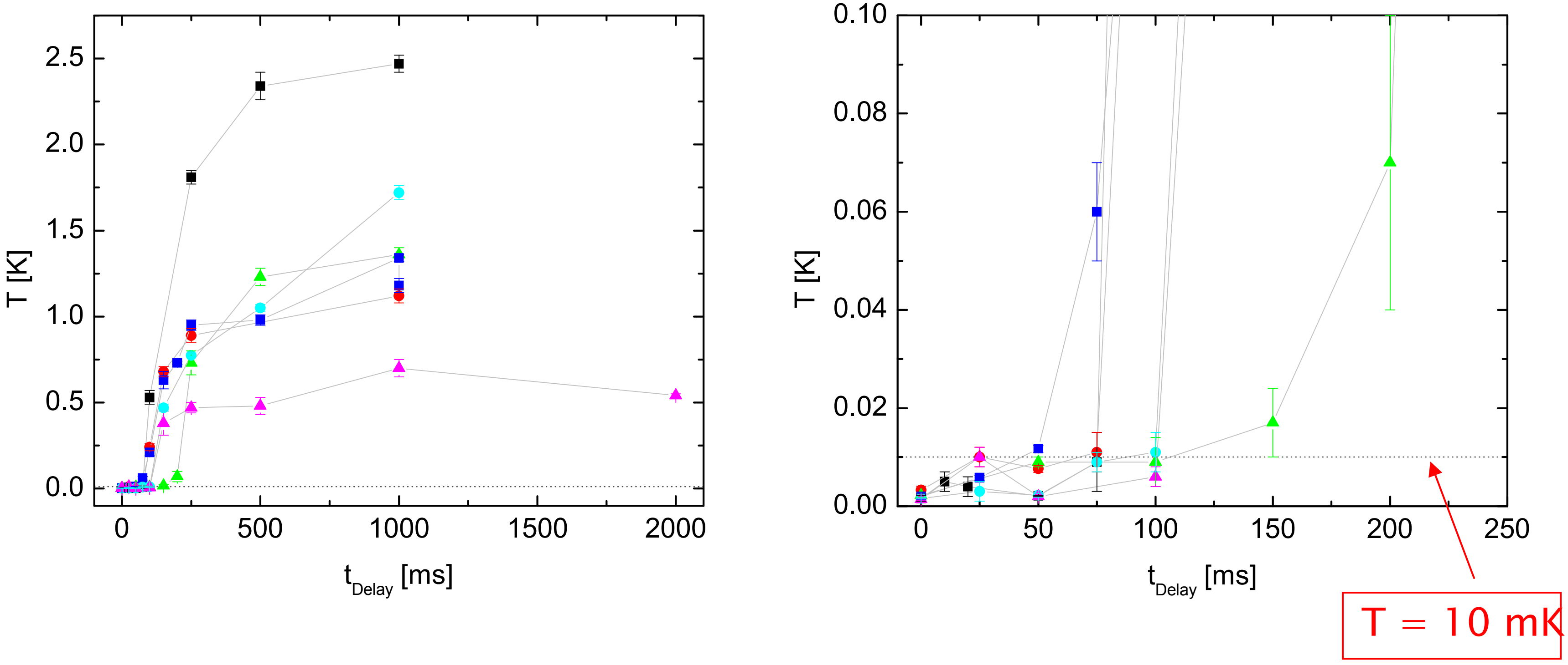

Onset of abnormal heating is at T = 10 mK
- the temperature of the solid-liquid phase transition
- but what is the explanation?

Pressure dependence

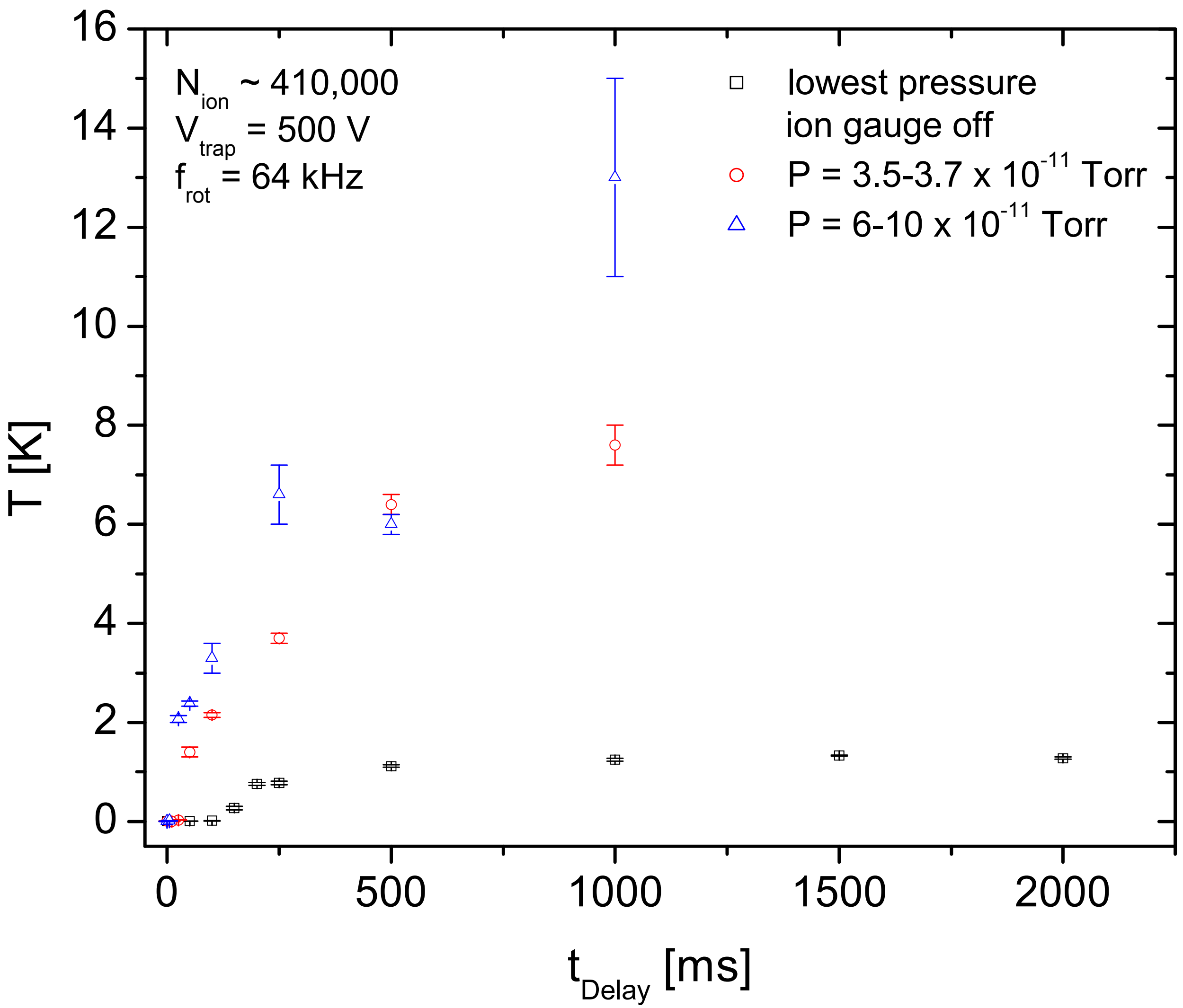

Clear correlation between pressure and heating!

Pressure increase ⇒ "step" occurs at earlier time
larger step

Heating rate measurements on a clean cloud of Be^+ ions

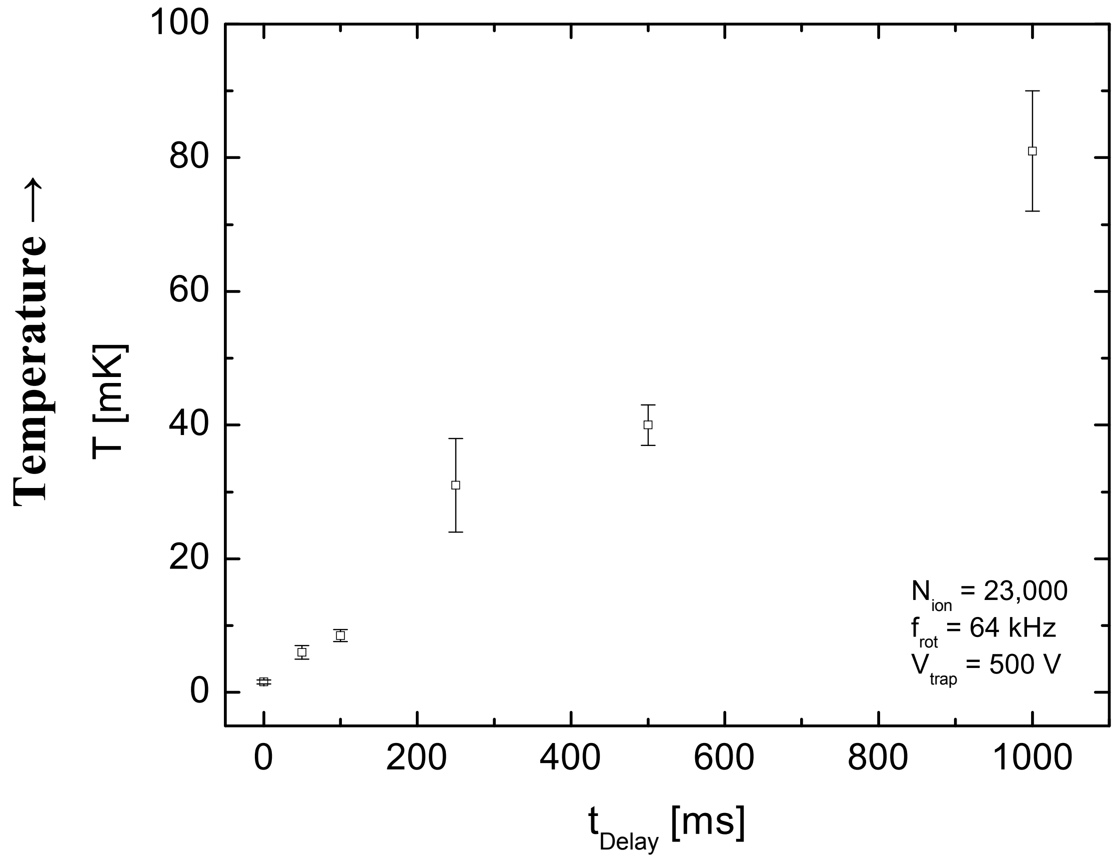

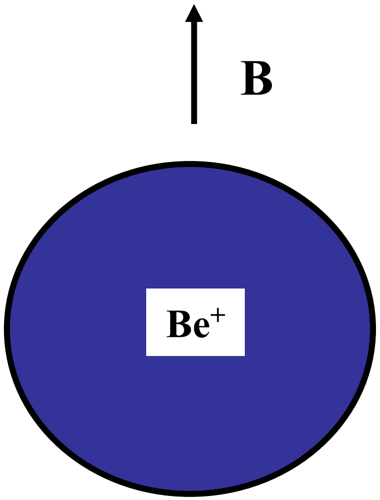

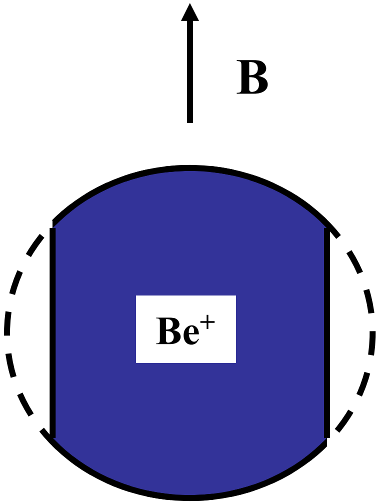

- **no anomalous heating at the solid-liquid phase transition!!**
- **anomalous heating requires heavy mass ions**

Sympathetic cooling of impurity ion cyclotron motion

- impurity ions heated by residual gas collisions; sympathetically cooled by laser-cooled Be^+ ions

$$\frac{dT_i}{dt} = r(T_i - T_{Be}) + h$$

T_i = impurity ion temperature

~0.1 K/s

- phase-locked control of ω_r ⇒ heavy ions crystallized ⇒ $T_i < 10$ mK

- but large magnetic field ⇒ $\mathbf{r_c = \langle v \rangle / \Omega_c \ll a_{WS}}$ ⇒ cyclotron motion decouples from parallel

- sympathetic cooling rate in crystalline state approximately given by (Dan Dubin, UCSD):

$$r_\perp \sim \frac{w_p^4}{\Omega_c^4}\gamma \sim 5 \times 10^{-4}\gamma$$ for impurity ion cyclotron motion

$$r_{||} \sim \gamma$$ for impurity ion motion parallel to **B**

γ = laser damping rate for Be^+ < 1 kHz for current experimental work

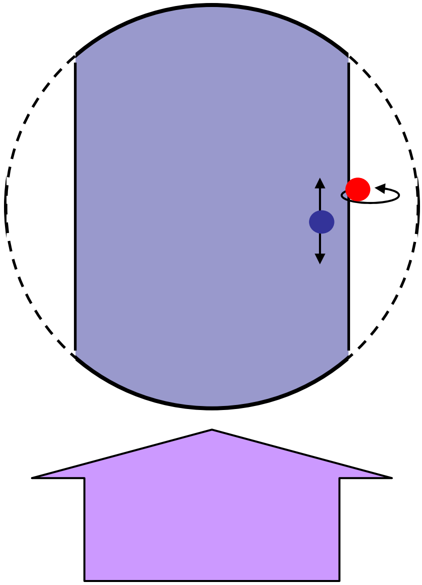

- h ~ 0.1 K/s, $r_?$ < 0.1 Hz ⇒ $T_{?,i} > 1$ K which is the correct order of magnitude to account for the observed heating

Impurity ion cyclotron motion drive increases the heating

T at 1 s vs rf drive frequency

heating with m=10 cyclotron drive

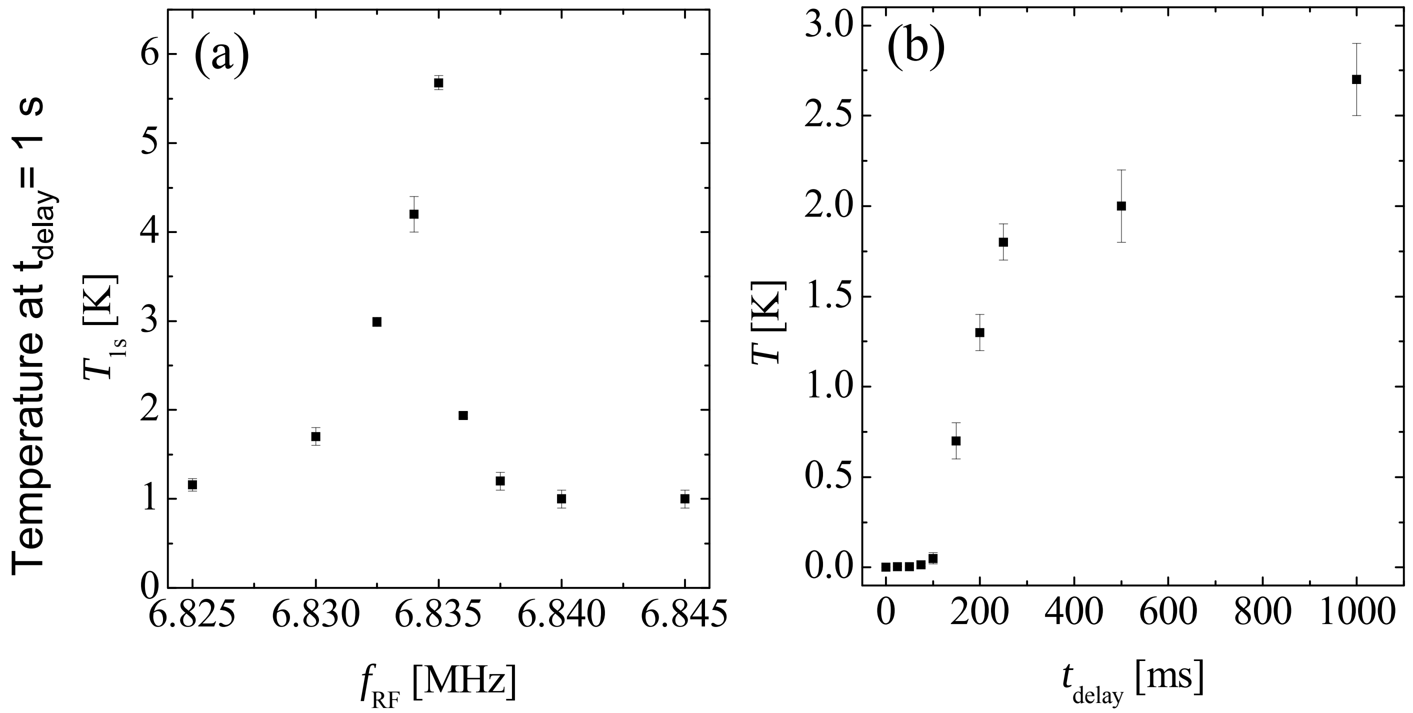

m=10 cyclotron drive frequency

Rapid heating explained by a release of the impurity ions cyclotron energy when the parallel ion temperature increases above 10 mK, the temperature of the solid-liquid phase transition.

Is there a theory for why the impurity ion cyclotron energy is released for T> 10 mK ?

Can we get rid of the heating?

Can we get rid of the heating?

- work with clean plasmas with no impurity ions
- stay in the liquid phase for as long as possible

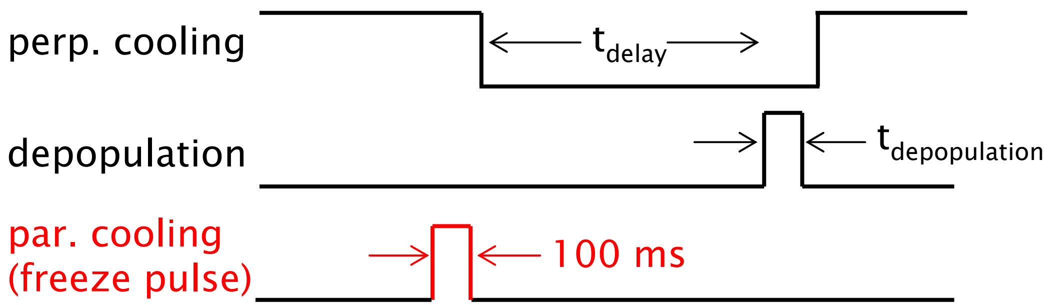

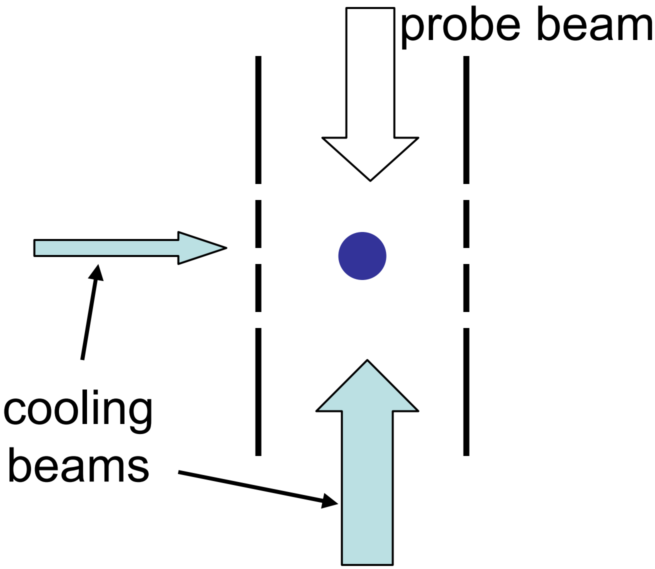

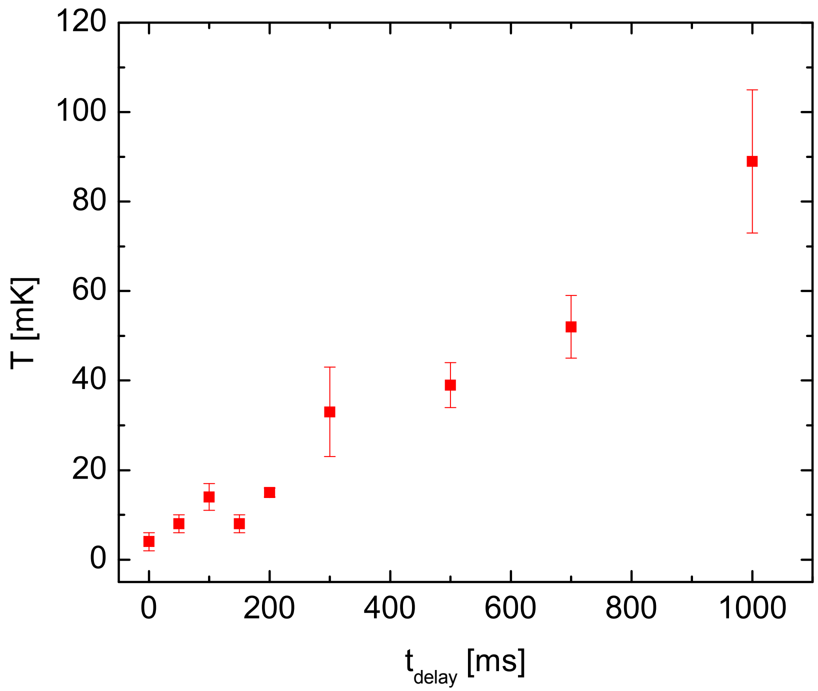

Plasma spends less than 100 ms in the solid phase prior to measurement
$\Rightarrow$ No additional energy is released at the solid-liquid phase transition

Is there a theory for why the impurity ion cyclotron energy is released for T> 10 mK ?

- **need a theory of perp/parallel energy equipartition**
- **such a theory exists in the absence of correlations (Γ < 1)**

O'Neil, Glinsky, Rosenbluth, Ichimaru,… (1992)

$$\frac{T_{\|}}{dt} = n_o \bar{v} \bar{b}^2 I(\bar{\kappa})(T_\perp - T_\|)$$

$$\bar{b} = \frac{2e^2}{k_B T_\|}, \bar{v} = \sqrt{\frac{2k_B T_\|}{m}},$$

$$\bar{\kappa} = \frac{\Omega_c \bar{b}}{\bar{v}} = \frac{\text{distance of closest approach}}{\text{cyclotron radius}}$$

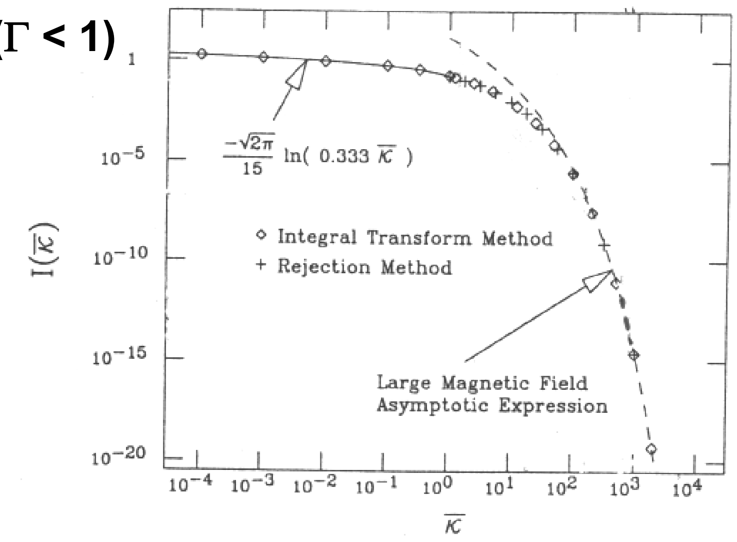

- O'Neil/Glinsky theory **is more than 10^7 too small to explain our observed heating rate**
- **rare close collisions between energetic particles are responsible for the equipartition**
- **close collisions can be enhanced in a correlated plasma where the Coulomb repulsion is screened by the neutralizing background**

Saltpeter and Van Horn, Astrophys. J **155** (1969) – **nuclear reaction rates in stellar interiors**

nuclear reaction rate (Γ > 1) ~ exp(Γ)£nuclear reaction rate(Γ<<1)

Summary of can we observe the phase transition?

- the first-order liquid-solid phase transition at Γ~170 has never been directly observed in an experiment.

- this should be possible by measuring the latent heat or possibly through Bragg scattering

- perp/parallel energy equipartition studies can measure the enhancement of close collisions for $\Gamma > 1$ for the first time

Plasma waves excited by laser radiation pressure

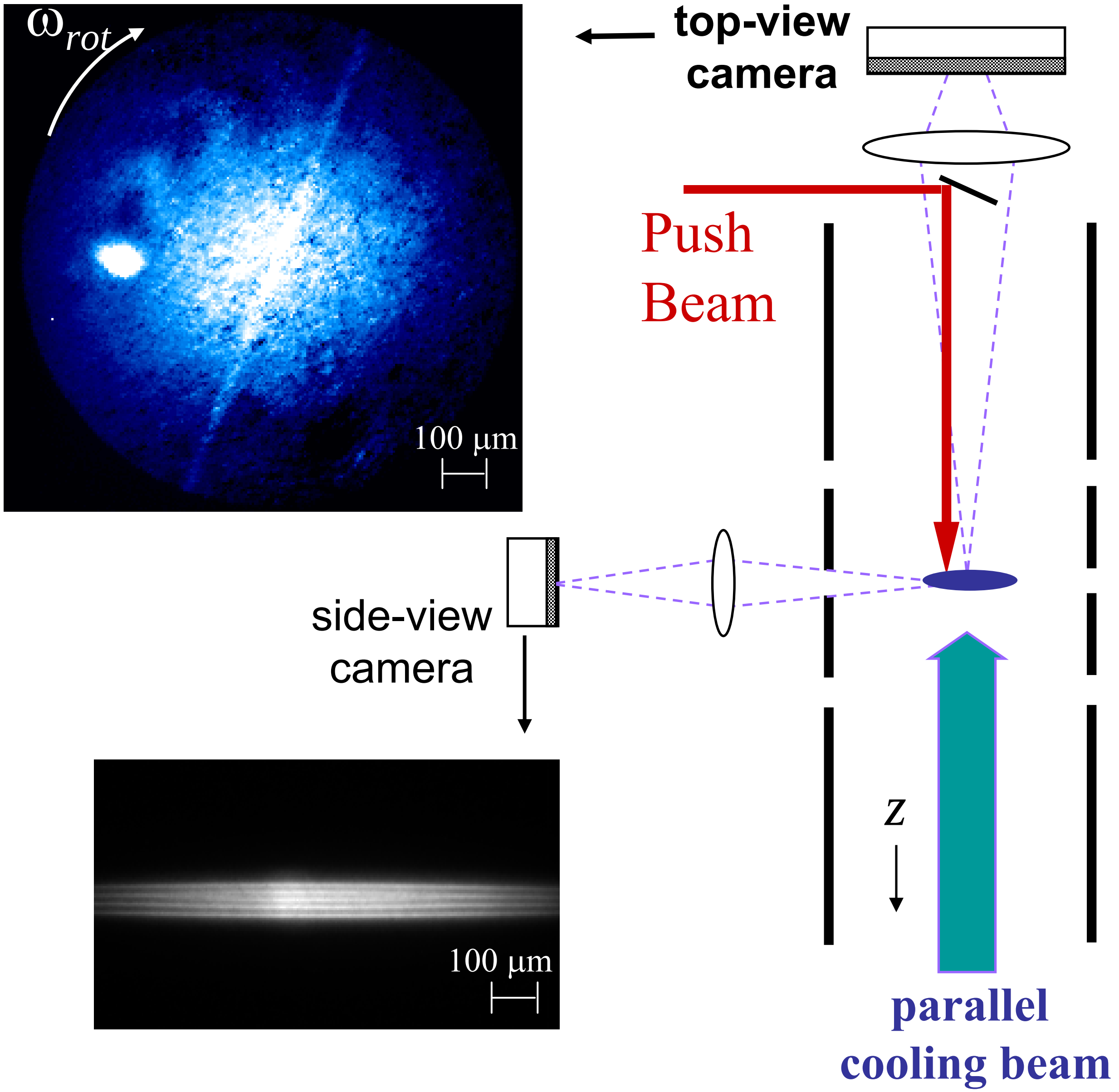

Push on the top of a rotating ion crystal with a laser beam.

The waves which are excited interfere to form a "wake".

Doppler image of wakes

Image w/ push beam

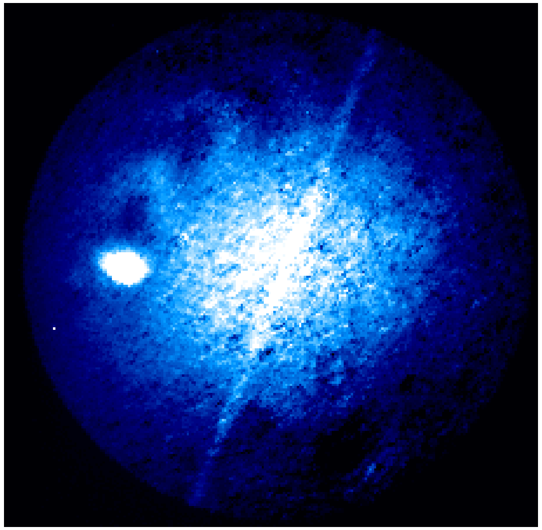

Image w/o push beam

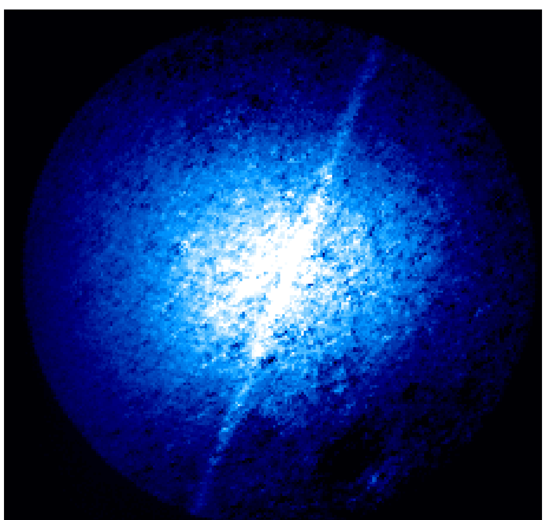

Subtract the two images

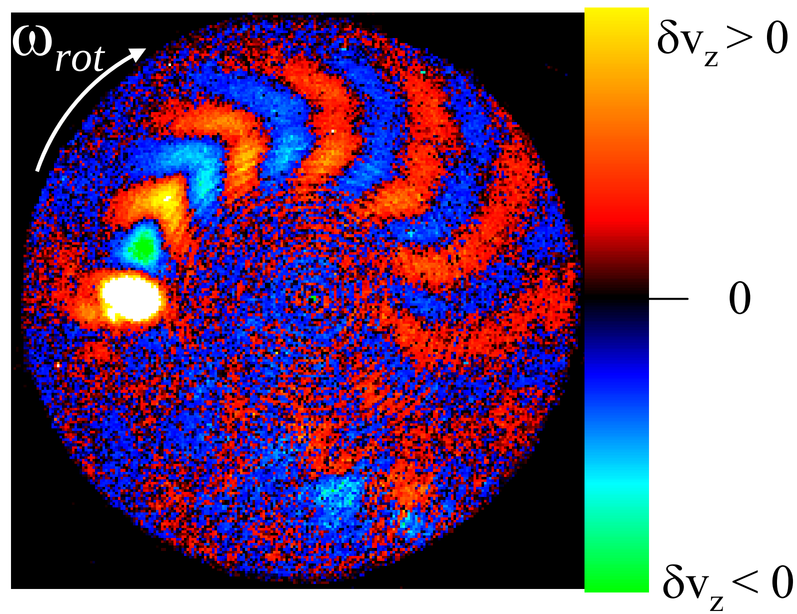

Variations in image intensity (shown with a false color scale) correspond to variations in the axial motion of the ions in the crystal.

A large spectrum of modes are excited, which interfere to form a wake that is stationary in the source (lab) frame.

Analogous to wakes in water

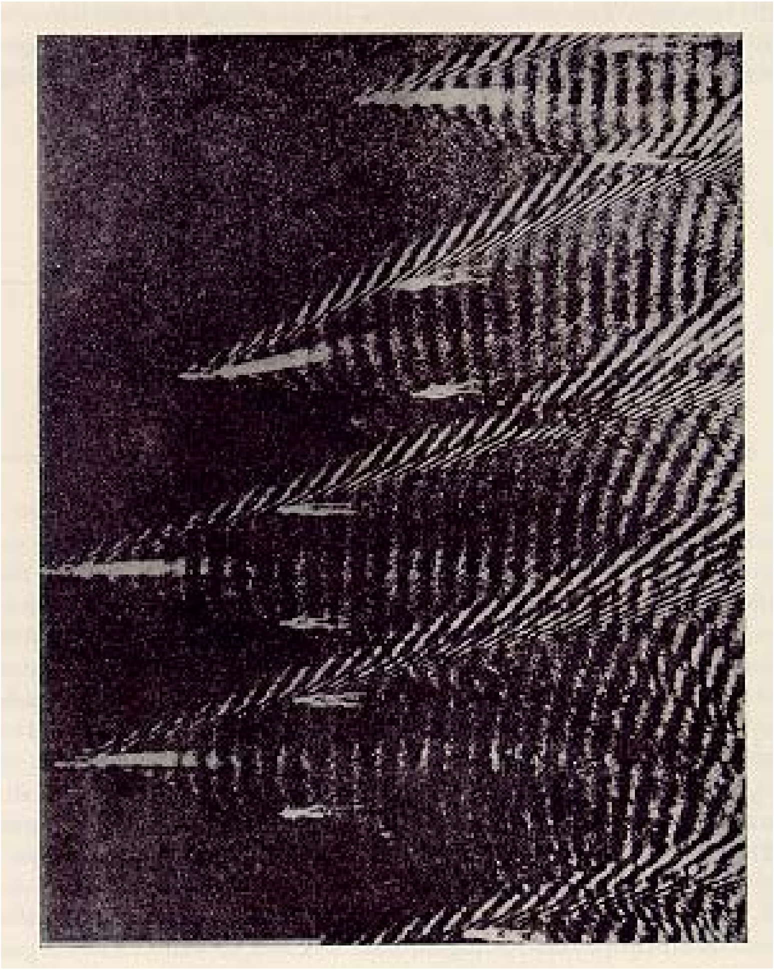

Wakes are Stationary in the frame of the source (ship).

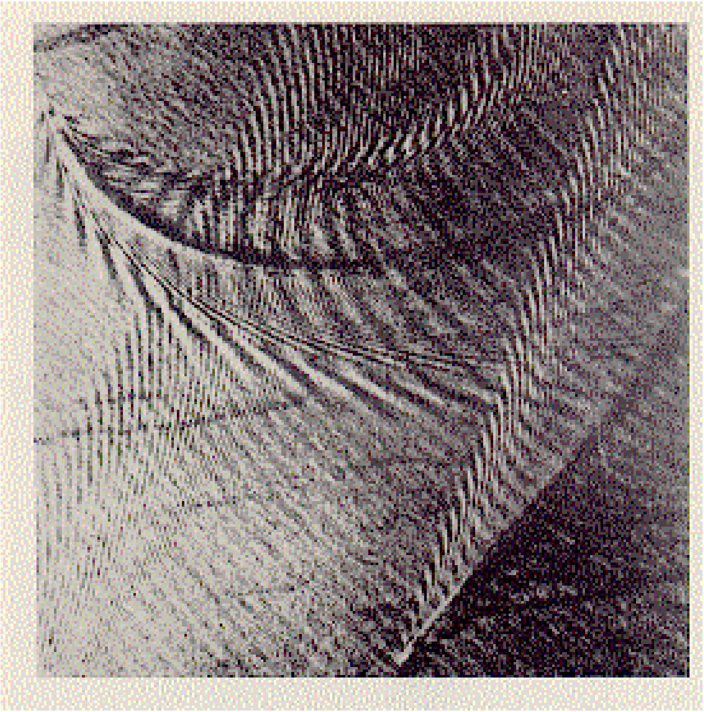

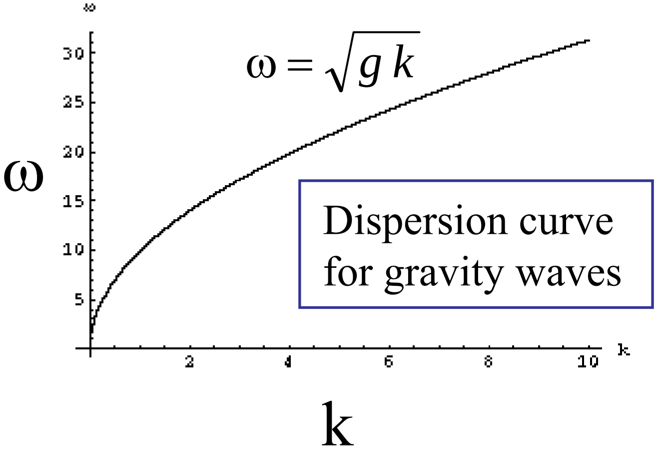

Dispersion curve for gravity waves

Analyze image to obtain λ and ω

Analyze wake pattern in an annular region that is directly "behind" the push beam.

Fit to damped sinusoid to get λ:

$$y = C_0 + C_1 \,\mathrm{Sin}(C_2 x + C_3)\, e^{-C_4 x}$$

$$C_2 = k = 2\pi/\lambda$$

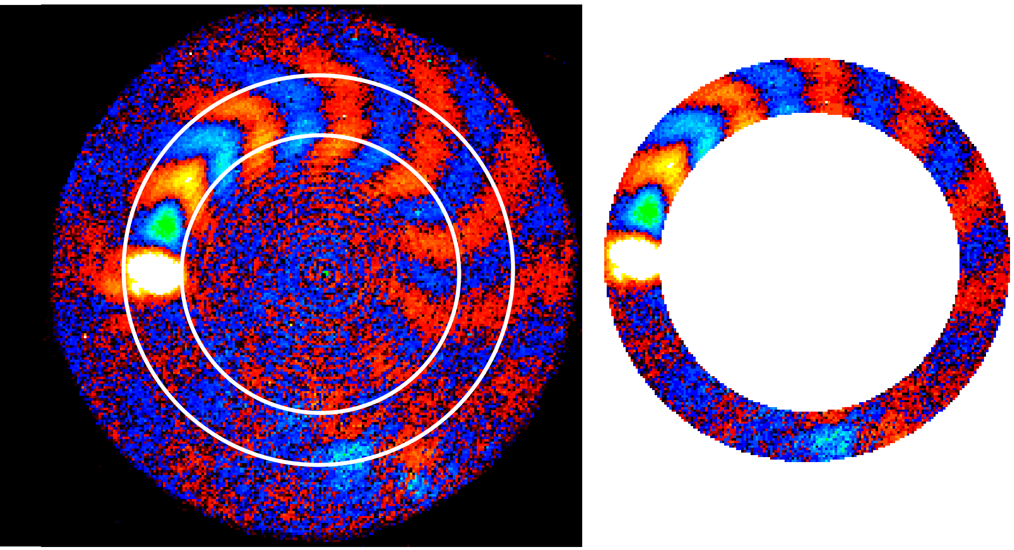

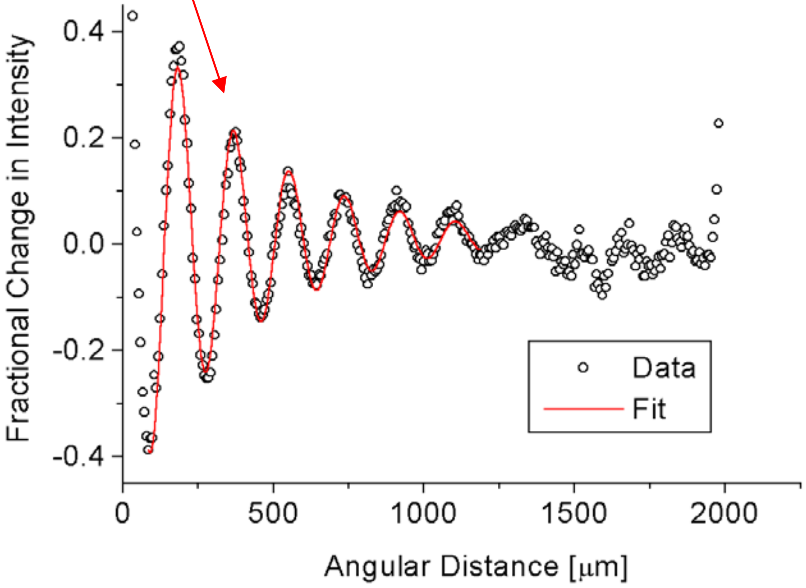

Directly behind the beam, the stationary phase condition gives:

$$v_{source} = \omega_{Rot}\, r_{source} = \omega/k$$

For this case:

$\lambda = 180\ \mu m$ $\quad\delta v_z < 1$ m/s

$\omega/2\pi = 500$ kHz $\quad\delta z < 0.3\ \mu m$

Dispersion relationship

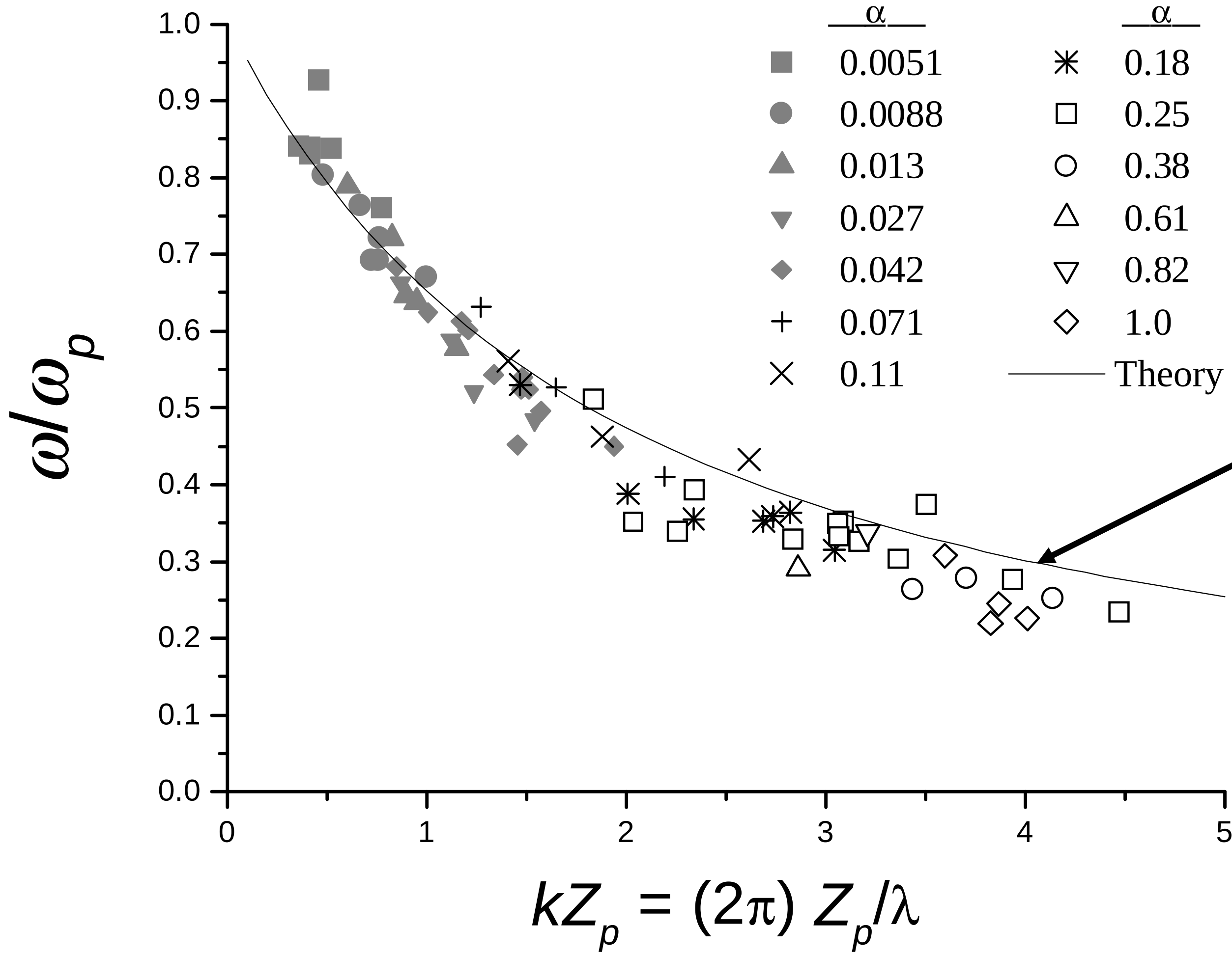

The data agrees with the theoretical dispersion relationship for drumhead waves in a plasma slab of thickness $2Z_p$.

$$\tan\left[\frac{kZ_p}{\sqrt{\omega_p^2/\omega^2 - 1}}\right] = \sqrt{\omega_p^2/\omega^2 - 1}$$

Theory replicates experiment

Side View

Top View

Experiment

Theory -Dubin

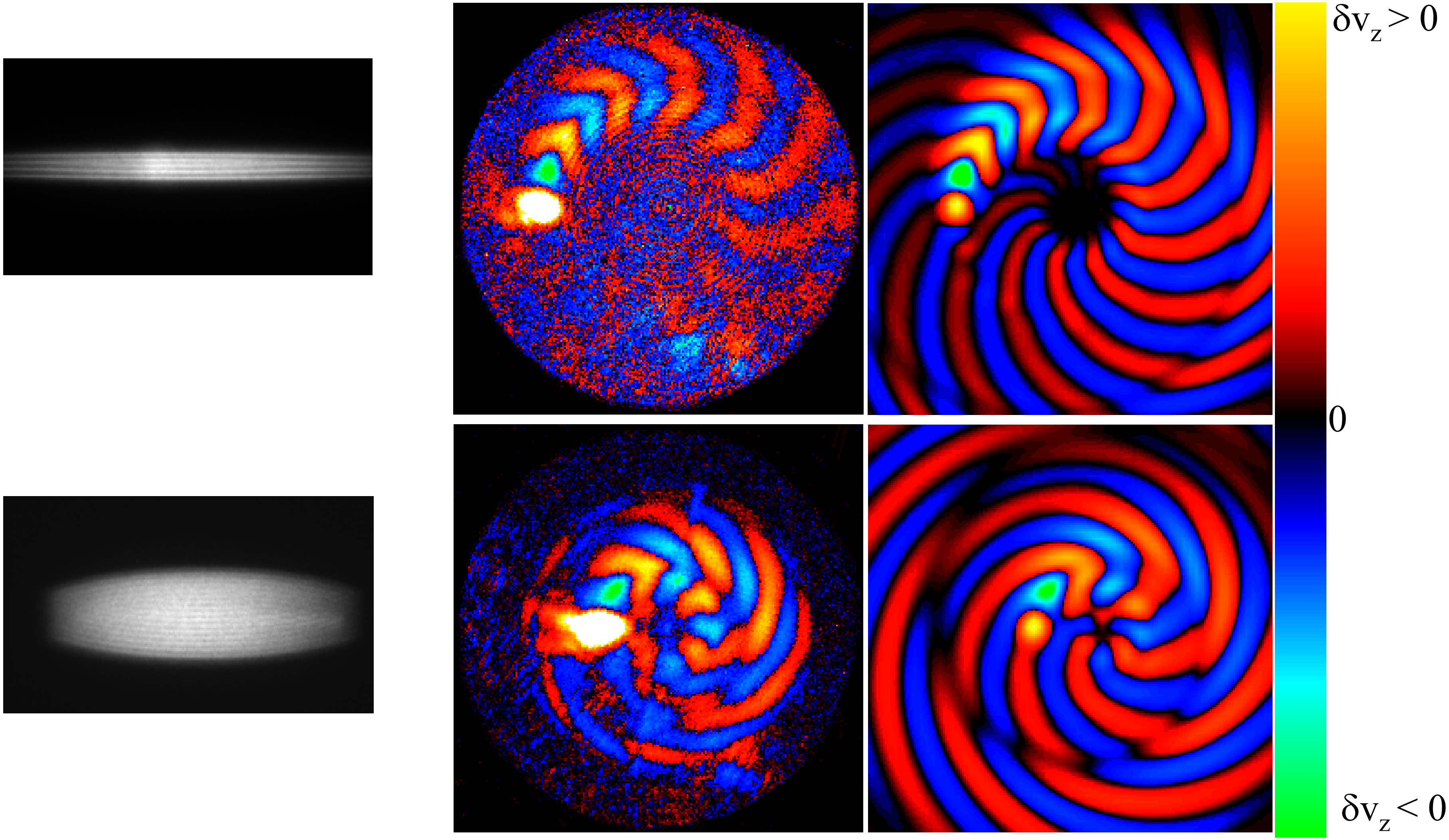

Future areas of work

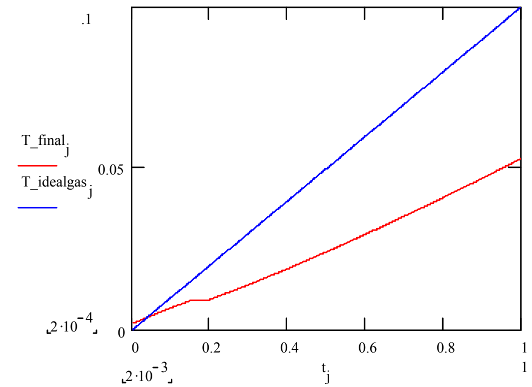

- Observation of the liquid-solid phase transition
- Studies of the enhancement of the perp/parallel equilibration due to strong correlation
- Shear modes

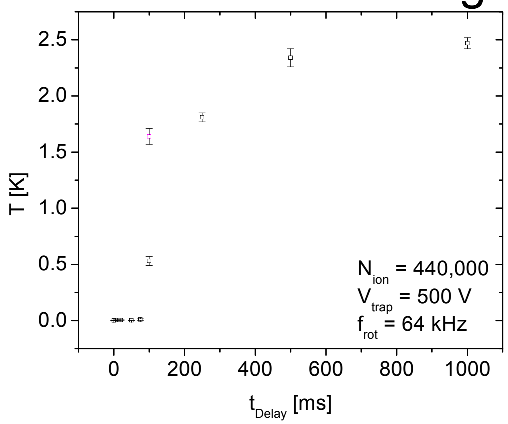

Application:

- Entangled states of trapped ions

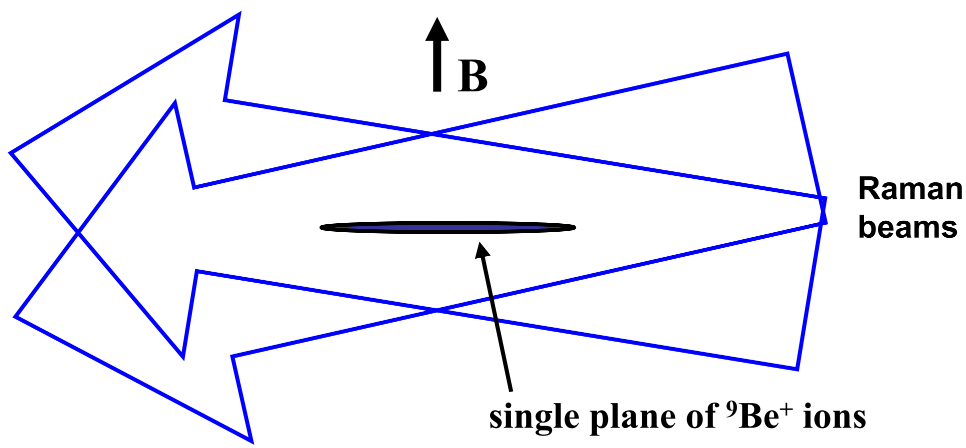

Deterministic entanglement through an $\exp(i\chi J_z^2 t)$ interaction